Control of anomalous diffusion of a Bose polaron

Christos Charalambous[1], Miguel Ángel García-March[1,2], Gorka Muñoz-Gil[1], Przemysław Ryszard Grzybowski[3], and Maciej Lewenstein[1,4]

[1]ICFO – Institut de Ciéncies Fotóniques, The Barcelona Institute of Science and Technology, 08860 Castelldefels (Barcelona), Spain

[2]Instituto Universitario de Matemática Pura y Aplicada, Universitat Politècnica de València, E-46022 València, Spain

[3]Faculty of Physics, Adam Mickiewicz University, Umultowska 85, 61-614 Poznań, Poland

[4]ICREA, Lluis Companys 23, E-08010 Barcelona, Spain

February 18, 2020

We study the diffusive behavior of a Bose polaron immersed in a coherently coupled two-component Bose-Einstein Condensate (BEC). We assume a uniform, one-dimensional BEC. Polaron superdiffuses if it couples in the same manner to both components, i.e. either attractively or repulsively to both of them. This is the same behavior as that of an impurity immersed in a single BEC. Conversely, the polaron exhibits a transient nontrivial subdiffusive behavior if it couples attractively to one of the components and repulsively to the other. The anomalous diffusion exponent and the duration of the subdiffusive interval can be controlled with the Rabi frequency of the coherent coupling between the two components, and with the coupling strength of the impurity to the BEC.

1 Introduction

The phenomenon of anomalous diffusion attracts a growing interest in classical and quantum physics, appearing in a plethora of various systems [1, 2]. In classical systems, there has been a considerable effort to elucidate the properties and conditions of anomalous diffusive behavior, with a large emphasis given to the question of how this anomalous diffusion could potentially be controlled. In many models, the appearance of the anomalous diffusion is attributed to some random component of the system-environment setup, usually distributed with a power-law. Examples include continuous time random walks [3], diffusion on a fractal lattice [4], diffusivity (i.e. diffusion coefficient) that is inhomogeneous in time [5, 6], or space [7–11] in a regular or random manner, the patch model [12, 13], hunters model [14], etc. In quantum systems, a paradigmatic instance of a highly controlled system is that of a Bose Einstein Condensate (BEC). It was shown that BEC with tunable interactions, are promising systems to study a number of diffusion-related phenomena, such as Anderson Localization (AL) in disordered media [15–17], the expansion of 1D BEC in disordered speckle potentials [15–23], the subdiffusive behavior of the expansion of a wave packet of a 1D quantum, chaotic and nonlinear system [15, 22, 24–33], the Brownian motion of solitons in BEC [34], as well as the superdiffusive motion of an impurity in a BEC studied in [35–37].

In this work, we study how an impurity in a coherently coupled two-component BEC shows a transient anomalous diffusing behavior. We study this phenomenon under experimentally relevant conditions, as long as the BEC can be approximated as uniform and one dimensional. We show that this transient anomalous diffusing behavior can be controlled through the strength of the interactions and the coherent coupling. To this end, we treat the Bose Polaron problem within an open quantum system framework. The open quantum system approach has been used recently in the context of ultracold quantum gases to study the diffusion of an impurity and two impurities in a BEC [35–37], for the movement of a bright soliton in a superfluid in one dimension [38], see also[39–41]). On the other hand, the effect of contact interactions, dipole-dipole interactions and disorder on the diffusion properties of 1D dipolar two-component condensates were studied in [42], identifying again the conditions for subdiffusion. The study of the diffusive behavior of a 2D two-component BEC in a disordered potential was undertaken in [43]. Finally, an important study on an impurity immersed in a two-component BEC was reported in [44].

The most important novel result of this work, is that we show that under certain assumptions, one can observe a transient subdiffusive behavior of the immersed impurity. We study this for experimentally feasible parameters, as long as the BEC can be approximated as uniform and one dimensional, and we examine how the strength of the coherent coupling and interactions modify this subdiffusive behavior.

To be more specific about the particularities of the system considered in this work, we assume that an external field drives the population transfer (spin-flipping) between the two atomic levels. The population transfer between the two levels turns out to be described by Josephson dynamics, leading to what is

known as internal Josephson effect (see e.g. [45]). This internal Josephson interaction controls the many-body physics of multicomponent phase coherent matter. Importantly, after diagonalizing the Hamiltonian through a Bogoliubov transformation, one obtains a spectrum that has two branches: the density mode, ungapped and with a linear behavior at low momenta; and the spin mode, gapped, with a parabolic behavior even at low momenta.

From the technical point of view, we identify how under suitable assumptions, starting from the Hamiltonian describing the aforementioned system of an impurity in a coherently coupled two component BEC, one can equivalently describe the impurity as a Brownian particle in a bath, where the role of the bath is played by the Bogoliubov modes of the coherently coupled two-component BEC. Furthermore, we show that the two branches obtained after the Bogoliubov transformation, the density mode and the spin mode, mentioned above, result in two distinct spectral densities, which we derive in Section 3. We consider two scenarios: same coupling among the impurity and the two bosonic components, and repulsive coupling to one component and attractive to the other. We show that these scenarios correspond to the impurity coupling either to the density or to the spin mode of the two-component BEC, respectively. For the coupling to the density mode there is no qualitative difference in comparison to the case where the impurity is embedded in a single BEC [35]. For the coupling to the spin mode, we find a different spectral density, namely a gapped sub-ohmic spectral density. We derive and solve the equations of motion of the impurity. These are obtained through the corresponding Heisenberg equations for the bath and impurity particles and they have the form of Generalized Langevin equations with memory effects. By solving numerically these equations we find the effect of the gapped sub-Ohmic spectral density on the Mean Square Displacement (MSD) of the impurity.

The paper is organized as follows. In Section 2 we introduce the model Hamiltonian and transform it into the form of a Caldeira-Leggett one. In Section 3 we derive the spectral densities for the cases of coupling to the density or spin modes. In Section 4 we find and solve the Langevin equations and in Section 5 we present the results. We end the paper with the discussion and outlook presented in Section 6.

2 Hamiltonian

The dilute Bose-Einstein condensates created in atomic gases [46] consist of bosons with internal degrees of freedom: the atoms can be trapped in different atomic hyperfine states. Soon after the first observation of atom trap BECs, experimentalists succeeded in trapping partly overlapping BECs of atoms in different hyperfine states that are (i) hyperfine split [47] or (ii) nearly degenerate and correspond to different orientations of the spin [48]. We consider a two-component Bose gas with both one-body (field-field) and two-body (density-density) couplings, composed of such atoms in different hyperfine states. Furthermore, we assume that the two components are coupled through a Josephson (one-body) type of coupling. The two-body interaction results from short-range particle-particle interactions between atoms in different internal states, while the one-body interaction can be implemented by two-photon Raman optical coupling, which transfers atoms from one internal state to the other. In present-day BEC experiments, the internal Josephson or Rabi interactions, interconverting atoms of different internal states, consist in two-photon transitions, induced by a laser field or a combination of a laser field and oscillating magnetic field. To gain a perspective on the experimental relevance of our study, we refer the readers to the work of Refs. [47, 49–51]. Finally, we assume an impurity that is immersed in the two-component BEC. This impurity interacts with both components through contact interactions. In Fig. 1 a sketch of the setup is shown.

The Hamiltonian of an impurity interacting with a two-species bosonic mixture in one dimension reads

$$H = H_{\mathrm{I}} + H_{\mathrm{B}}^{(1)} + H_{\mathrm{B}}^{(2)} + H_{\mathrm{IB}} + H_{\mathrm{B}}^{(12)}, \qquad (1)$$

where the impurity of mass m_{I} is described by $H_{\mathrm{I}} = \frac{\mathbf{p}^2}{2m_{\mathrm{I}}} + U(\mathbf{x})$, with $U(\mathbf{x})$ being the trapping potential. The interactions with the bosons are described by H_{IB}. We study here only the case of free impurities, hence we assume $U(\mathbf{x}) = 0$. The terms of the individual bosonic species, labeled with the index $j = 1, 2$, are

$$H_{\mathrm{B}}^{(j)} = \int \Psi_j^\dagger(\mathbf{x}) \left[-\frac{\mathbf{p}_j^2}{2m_{\mathrm{B}}^j} + V^j(\mathbf{x}) \right] \Psi_j(\mathbf{x})\, \mathrm{d}\mathbf{x} + \frac{g_j}{2} \int \Psi_j^\dagger(\mathbf{x})\, \Psi_j^\dagger(\mathbf{x})\, \Psi_j(\mathbf{x})\, \Psi_j(\mathbf{x})\, \mathrm{d}\mathbf{x},$$

where the intra-species contact interactions have a strength given by the coupling constant $g_j = 4\pi\hbar^2 a_{\mathrm{B}}^{(j)}/m_{\mathrm{B}}^j$, with $a_{\mathrm{B}}^{(j)}$ the scattering length for the j^{th} species atoms, m_{B}^j the mass of the atoms of these species and the external potential for the atoms of the j^{th} species is denoted by $V^j(x)$. For simplicity, we assume $V^1(x) = V^2(x) = V(x)$ and $m_{\mathrm{B}}^1 = m_{\mathrm{B}}^2 = m_{\mathrm{B}}$. Furthermore we focus on the idealized case of an untrapped bath i.e. $V(x) = 0$ which results in a homogeneous density for the BEC. This is not a physical scenario, but in practice, for a BEC trapped in a large box, the impurity in the middle of this box would indeed approximately interact with a bath of constant density.

The coupling Hamiltonian between the two bosonic species consists in inter-species contact interactions, with coupling constant g_{12}, and a Rabi coupling Ω,

which exchanges atoms between components, i.e.,

$$H_{\mathrm{B}}^{(12)} = g_{12} \int \Psi_1^\dagger(\mathbf{x})\, \Psi_2^\dagger(\mathbf{x})\, \Psi_2(\mathbf{x})\, \Psi_1(\mathbf{x})\, \mathrm{d}\mathbf{x} + \hbar\mathbf{\Omega} \int \Psi_1^\dagger(\mathbf{x})\, \Psi_2(\mathbf{x})\, \mathrm{d}\mathbf{x} + \mathrm{H.c.} \quad (2)$$

where $g_{12} = 4\pi\hbar^2 a_{\mathrm{B}}^{(12)}/m_{\mathrm{B}}$, with $a_{\mathrm{B}}^{(12)}$ the scattering length for the intraspecies interactions. Without any loss of generality, we will only consider $\mathbf{\Omega}$ real and positive. This is because even if a complex Rabi frequency is assumed, this can always be cancelled by introducing a counteracting phase for one of the BECs, which can be shown to have no effect on the energy spectrum of the bath. The latter part of the Hamiltonian, referred to as an internal Josephson interaction, is a two-photon transition that is induced by a laser field or a combination of a laser field and an oscillating (rf) magnetic field. This also introduces an effective energy difference between the two internal states/species of the BEC, which, assuming a low intensity driving field, is simply equal to the detuning δ of the two-photon transition. This detuning does not affect our studies however, so for sake of clarity and simplicity, we will assume it to be zero. We also consider here only repulsive two-body coupling, i.e. $g_{12} > 0$.

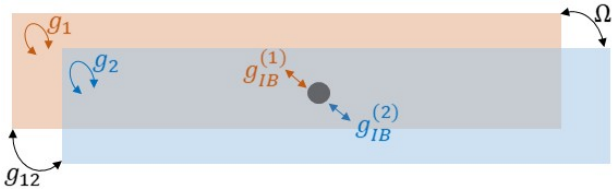

Figure 1: We consider a setup of a coherently coupled two-component BEC in which an impurity is immersed. By g_1 and g_2 we denote the intraspecies contact interactions of the atoms of the first and second species respectively. g_{12} refers to the coupling strength of the interspecies contact interaction among atoms of the first and second species. By Ω we denote the Rabi frequency of the Raman coherent coupling between the two species. Finally $g_{IB}^{(1)}$ and $g_{IB}^{(2)}$ indicate the coupling of the impurity to the atoms of the first and second species respectively.

In what concerns the impurity-bosons interaction part of the Hamiltonian, we assume that the interaction is between the impurity and the densities of the bosons, i.e. it has the form of a contact interaction:

$$H_{\mathrm{IB}} = \left(\sum_{j=1,2} g_{\mathrm{IB}}^{(j)} \Psi_j^\dagger(\mathbf{x}) \Psi_j(\mathbf{x}) + h.c. \right). \quad (3)$$

with $g_{\mathrm{IB}}^{(j)} = 2\pi\hbar^2 a_{\mathrm{IB}}^{(j)}/m_{\mathrm{R}}$, where $a_{\mathrm{IB}}^{(j)}$ represents the scattering length of the impurity with the bosons of the j^{th} BEC, and $m_{\mathrm{R}} = m_{\mathrm{B}} m_{\mathrm{I}}/(m_{\mathrm{B}} + m_{\mathrm{I}})$ is the relevant reduced mass. From this point onwards, we assume that the BEC is one dimensional, which simplifies the analytical part of our studies. Nevertheless, the main result of our work, which is the control of the dynamics of an impurity in a coherently coupled two-component BEC by coupling it either to the density mode of the BEC or to the spin mode of the BEC, will remain irrespective of the dimension. The diffusing behavior itself however might change, since the spectral density depends on the dimension of the BEC. It is worth noting here, that the 1D case in fact is peculiar since, in principle, in the purely 1D scenario (not in the confined 3D elongated/cigar shaped case) the condensation is destroyed by the phase fluctuations [52]. However, if the phase coherence length is larger than the band-size, then one can speak about "true" BEC. In other words, as long as the physics of interest happens on the scales smaller than the phase coherence length, it is legitimate to use BEC and Bogolubov-de Gennes theory, as we will do in our work.

Furthermore, we comment here that, had we considered the more realistic case of a harmonically trapped BEC, assuming it to be described by a Thomas-Fermi density profile, this would lead to a discretized Bogoliubov spectrum, which would then have to be treated under a similar approximation as in the single BEC case in [36]. In principle, we expect that the maim result of this work, i.e. being able to couple the impurity to two distinct types of baths, should hold, but the related diffusing behaviours might change. We expect that when the gap of the spin models is much bigger than the trap frequency, the sub-diffusion, that we observe in Sec. 5, should persist in the same form. The reader should also have in mind that, as discussed in the appendix of [36] the limit of the trapping frequency of the BEC going to 0 would not lead to the homogeneous BEC case. This scenario requires a more careful treatment, that goes beyond the scope of our paper.

A further assumption we make in our studies is that of a dilute gas of low depletion, since in this case, we will be able to apply the Bogoliubov diagonalization technique and obtain the energy spectrum of the BEC bath. In the low-density sub-milikelvin temperature regime of the atom trap experiments, we may assume that the trapped atoms interact only through the partial s-wave channel, and that the many-body properties are well described by assuming the particles to interact as hard spheres. The radius of those spheres is given by the scattering length a, which we assume to be positive. We say that the system of particle density n is dilute if the packing fraction of space occupied by the spheres $na^3 \ll 1$. The assumption of low depletion means that almost all particles occupy, on average, the single particle state associated with the condensate ($k = 0$, where k is the momentum for the particular case of homogeneous BEC that we will be considering). This implies that the temperatures to be considered should be smaller than the critical temperature.

For a single BEC, all the bosons condensate at the same state. However, this will not be the case for the two-component BEC and one has to determine the fraction of particles in each component, which will depend on the ground state of the system. This is determined by the parameters of the system.

With the above considerations in mind, we assume that the two bosonic gases condense. This means that we can apply mean field theory and further assuming that the ground state is coherent, the wavefunctions $\Psi_j(x), \Psi_j^\dagger(x)$ for a homogeneous BEC are given by

$$\Psi_j(x) = \Psi_{j,0}(x) + \delta\Psi_j(x), \tag{4}$$

where $\Psi_{j,0}(x) = \phi_0(x)\sqrt{N_j}e^{i\theta_j}$, with θ_j being the phase of the coherent j^{th} component, N_j the number of bosons of the j^{th} species and $\delta\Psi_j(x) = \sum_{k\neq 0}\phi_{j,k}(x)a_{j,k}$ with $\phi_k(x) = \frac{1}{\sqrt{V_j}}e^{ikx/\hbar}$ the plane wave solutions, with V_j the corresponding bath's volume. From here onwards we assume for simplicity that $V_1 = V_2 = V$, i.e. that the two baths have the same volume, and that we are dealing with homogeneous BECs. Here $a_{j,k}$ and $a_{j,k}^\dagger$ are bosonic annihilation and creation operatos. To proceed further, we write the Hamiltonian in terms of these operators. The bosonic parts read

$$\begin{aligned} H_{\mathrm{B}}^{(j)} &= \sum_k \epsilon_k a_{j,k}^\dagger a_{j,k} \\ &\quad + \frac{g_j}{2}\sum_{k,k',q} a_{j,k+q}^\dagger a_{j,k'-q}^\dagger a_{j,k}a_{j,k'}, \\ H_{\mathrm{B}}^{(12)} &= g_{12}\sum_{k,k',q} a_{1,k+q}^\dagger a_{2,k'-q}^\dagger a_{2,k}a_{1,k'} \\ &\quad + \hbar\Omega\sum_k a_{1,k}^\dagger a_{2,k} + \mathrm{H.c.}, \end{aligned}$$

with $\epsilon_k = k^2/2m_{\mathrm{B}}$. The zeroth order expectation value (or mean field value) of the Hamiltonian reads as

$$\begin{aligned} H_0 &= \sum_j \frac{g_j}{2V}\Psi_{j,0}^4 + \frac{g_{12}}{V}\Psi_{1,0}^2\Psi_{2,0}^2 \\ &\quad + \hbar\Omega\left(\Psi_{1,0}(\Psi_{2,0})^* + (\Psi_{1,0})^*\Psi_{2,0}\right) \end{aligned} \tag{5}$$

2.1 Generalized Bogoliubov transformation

We now perform a generalized Bogoliubov transformation to diagonalize the Bosonic part of the Hamiltonian and hence obtain the energy spectrum of the bath. We follow closely the results of [53–55] in the rest of this section. This generalized Bogoliubov transformation is understood to be composed of a rotation, a scaling and one more rotation as in [53]. The derivation is based on a simple geometrical picture which results in a convenient parametrization of the transformation. Following the generalized Bogoliubov transformation, the initial bath operators are transformed as

$$\begin{aligned} a_{j,k} &= \mathcal{Q}_{j,+,k}^0 b_{+,k} + \mathcal{Q}_{j,+,k}^1 b_{+,-k}^\dagger \\ &\quad + (-1)^{\delta_{j,-}}\left(\mathcal{Q}_{j,-,k}^0 b_{-,k} + \mathcal{Q}_{j,-,k}^1 b_{-,-k}^\dagger\right) \\ a_{j,-k}^\dagger &= \mathcal{Q}_{j,+,k}^1 b_{+,k} + \mathcal{Q}_{j,+,k}^0 b_{+,-k}^\dagger \\ &\quad + (-1)^{\delta_{j,-}}\left(\mathcal{Q}_{j,-,k}^1 b_{-,k} + \mathcal{Q}_{j,-,k}^0 b_{-,-k}^\dagger\right), \end{aligned} \tag{6}$$

with $b_{+(-),k}^\dagger$ and $b_{+(-),k}$ and the creation/annhilation operators for the final spin (+) and density or phonon (−) mode. In the latter, the total density fluctuates, while in the spin mode (+) the unlike particle densities fluctuate out of phase. This, in the presence of an internal Josephson interaction as in our case, is a Josephson plasmon [56]. In Eq. (6) the parameters are as follows: $\delta_{1(2),-(+)} = 1$, $\delta_{1(2),+(-)} = 0$ and

$$\begin{aligned} &\mathcal{Q}_{j,s,k}^\phi = \\ &R_{sj}\hat{\Gamma}_{j,s,k}\Big[(1-\delta_{j,s})\cos(\gamma_k) + \delta_{j,s}\sin(\gamma_k)\Big]\cos\theta \\ &+ R_{sj'}\hat{\Gamma}_{j',s,k}\Big[(1-\delta_{j',s})\cos(\gamma_k) + \delta_{j',s}\sin(\gamma_k)\Big]\sin\theta, \end{aligned} \tag{7}$$

where $j' \neq j$, $\phi \in \{0,1\}$, $s \in \{+,-\}$, $\hat{\Gamma}_{j(j'),s,k} = [\Gamma_{j(j'),s,k}^2 + (-1)^\phi]/2\Gamma_{j(j'),s,k}$ and $R_{1+} = R_{2-} = (1,-1)^\top$, $R_{2+} = -R_{1-} = (1,1)^\top$. Also, in Eq. (7),

$$\begin{aligned} &\sin(\gamma_k) = \\ &\sqrt{\frac{1}{2}\left[1 - \frac{[\omega_{1,k}^2 - \omega_{2,k}^2]}{\sqrt{(\omega_{1,k}^2 - \omega_{2,k}^2)^2 + 16\Lambda_{12}^2 n_1 n_2 e_{1,k}e_{2,k}}}\right]}, \end{aligned} \tag{8}$$

with $\cos(\gamma_k)$ defined accordingly, and $\Gamma_{j,s,k} = \sqrt{e_{j,k}/E_{s,k}}$ where

$$\begin{aligned} &E_{\pm,k} := \hbar\Omega_{\pm,k} = \\ &\left[\frac{\sum_j \omega_{j,k}^2 \pm \sqrt{(\omega_{1,k}^2 - \omega_{2,k}^2)^2 + 16\Lambda_{12}^2 n_1 n_2 e_{1,k}e_{2,k}}}{2}\right]^{\frac{1}{2}}, \end{aligned} \tag{9}$$

with

$$\begin{aligned} e_{j,k} &= \epsilon_k - (-1)^j\frac{\left(1+(-1)^j\cos\theta_{12}\right)\hbar\Omega n}{2n_1 n_2} \\ \omega_{j,k} &= \sqrt{e_{j,k}^2 + 2\Lambda_j n_j e_{j,k}}, \\ \Lambda_1 n_1 &= g_1 n_1\cos^2(\theta) \\ &\quad + g_2 n_2\sin^2(\theta) + g_{12}\sin(2\theta)\cos(\theta_{12}), \\ \Lambda_2 n_2 &= g_1 n_1\sin^2(\theta) \\ &\quad + g_2 n_2\cos^2(\theta) - g_{12}\sin(2\theta)\cos(\theta_{12}), \\ \Lambda_{12}\sqrt{n_1 n_2} &= \frac{g_2 n_2 - g_1 n_1}{2}\sin(2\theta) \\ &\quad + g_{12}\sqrt{n_1 n_2}\cos(2\theta)\cos(\theta_{12}), \end{aligned}$$

where $n_j = \frac{N_j}{V}$ is the particle density of the j^{th} bath, and θ is the free parameter (angle) to be determined

by the minimisation of the total energy. In the above expression, $\theta_{12} = \theta_1 - \theta_2$ is the relative phase between the two BEC. The minimization of the zeroth energy with respect to the angle θ gives

$$\tan(\theta) = \begin{cases} \sqrt{\frac{n_1}{n_2}}, & \text{if } \theta_{12} = \pi, \\ \sqrt{\frac{n_2}{n_1}}, & \text{if } \theta_{12} = 0. \end{cases} \tag{10}$$

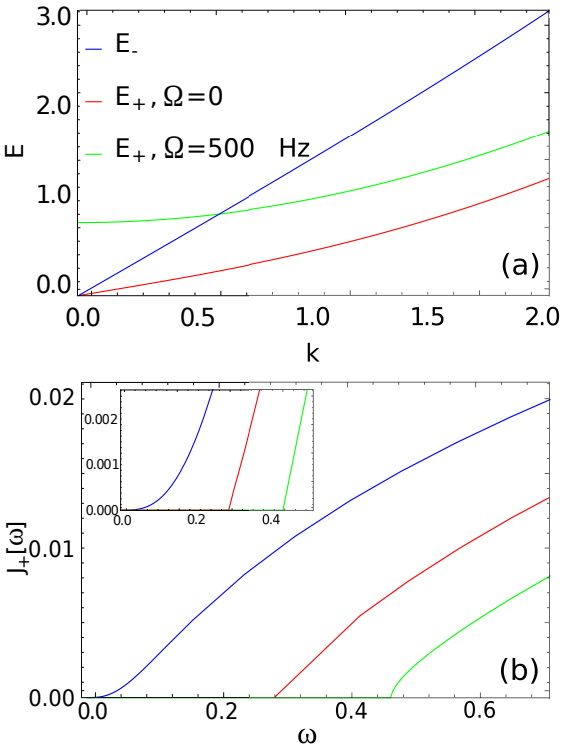

Figure 2: (a) Energy spectrum for a coherently coupled two component BEC. There are two branches in the spectrum corresponding to the density (-) and spin modes (+). We plot both for different values of the coherent coupling, Ω. First, this illustrates that the gap opens for the spin mode (+); and second, it shows that, while for $\Omega = 0$ both branches behave similarly, i.e., linearly for low k and quadratically for large k, for finite Ω the (+) mode behaves quadratically even at low k. This has direct implications on the behavior of the spectral density in case 2, plotted in (b). When the $\Omega = 0$ (blue line) the spectral density behaves as for the density mode (i.e. with a w^3-behavior). The red and green lines (for $\Omega = 50\pi, 100\pi$Hz, respectively) show instead a different behavior. The inset shows a zoom, where we checked that it fits the simplified behavior in Eq. (50), i.e. has a lower gap and behaves as $\sqrt{\omega}$ initially. In these plots we used $g = g_{12} = 2.15 \times 10^{-37} J \cdot m$, $n = 7(\mu m)^{-1}$, $g_{\rm IB} = 0.5 \times 10^{-37} J \cdot m$, with BEC and impurities made of Rb and K atoms, respectively.

By minimizing with respect to the population imbalance $f = \frac{N_1 - N_2}{N}$, one can obtain the following conditions on the parameters of the system in order to have an extremum of the energy,

$$\Delta + Af - \cos\theta_{12} \frac{f}{(1-f^2)^{1/2}} = 0, \tag{11}$$

where $A = \frac{(g_1+g_2-2g_{12})n}{4\hbar\Omega}$ is the mutual interaction parameter, $\Delta = \frac{2\delta+(g_1-g_2)n}{4\hbar\Omega}$ is the effective detuning parameter, and

$$A - \cos\theta_{12} \frac{1}{(1-f^2)^{3/2}} > 0, \tag{12}$$

is the condition to have a minimum of the energy. In [53], it was shown that to obtain the minimum energy of the system, without imposing any condition on the detuning δ, as is our case, then the relative phase should be chosen to be $\theta_{12} = \pi$, referred to as the π-state configuration. From here on we assume the symmetric case, i.e, $g_1 = g_2 = g$ as this will allow us to obtain analytically the spectral density in section 3. In this case, the equilibrium condition Eq. (11) reads as

$$\left(g - g_{12} + \frac{\hbar\Omega}{\sqrt{n_1 n_2}}\right)(n_1 - n_2) = 0, \tag{13}$$

which has two solutions

$$\begin{aligned} n_1 - n_2 &= 0 && \text{(GS1)}, \\ n_1 - n_2 &= \pm n\sqrt{1 - \left(\tfrac{2\hbar\Omega}{(g-g_{12})n}\right)^2} && \text{(GS2)}, \end{aligned} \tag{14}$$

corresponding to neutral GS1 and polarized ground states GS2. Here, we make the strong Josephson junction assumption

$$|A| < 1, \tag{15}$$

which is also referred to as the *miscibility condition*. This implies that the minimum energy equilibrium ground state has to be GS1 as is shown in [53, 55]. Handable expressions for the spectral density obtained section 3 are possible over GS1. For the regime in which ground state is GS2 we expect similar qualitative behavior, but we did not obtained a form for the spectral density which allows us to obtain the diffusive behavior of the impurity. The study of the impurity diffusion over GS2, and even at the phase transition, falls out of the scope of this paper. Under the miscibility condition (15), the energy spectrum expressions simplifies into

$$E_{-,k} = \left(\epsilon_k \left(\epsilon_k + (g + g_{12})\, n\right)\right)^{\frac{1}{2}}, \tag{16}$$

$$E_{+,k} = \left[\epsilon_k \left(\epsilon_k + (g - g_{12})\, n + 4\hbar\Omega\right) + 2\hbar\Omega \left[(g - g_{12})\, n + 2\hbar\Omega\right]\right]^{\frac{1}{2}}. \tag{17}$$

In Fig. 2 we plot the energy spectra as a function of k for specific parameters, to illustrate the spin and density branches. Furthermore, note that the bogoliubov transformation elements satisfy the well-known relation

$$\mathcal{Q}_k^0 (\mathcal{Q}_k^0)^T - \mathcal{Q}_k^1 (\mathcal{Q}_k^1)^T = 1, \tag{18}$$

where $\mathcal{Q}_k^\phi = \begin{pmatrix} \mathcal{Q}^\phi_{1,+,k} & \mathcal{Q}^\phi_{1,-,k} \\ \mathcal{Q}^\phi_{2,+,k} & \mathcal{Q}^\phi_{2,-,k} \end{pmatrix}$ with $\phi \in \{0, 1\}$, that implies normalization. However, as is shown in

[54], these Bogoliubov operators, do not fulfill the bosonic commutations relations, which is understood as a consequence of the fact that they are not orthogonalized with respect to the quasicondensate functions $\Psi_{j,0} = \sqrt{N_j} e^{i\theta_j}$. In [54] it is shown that to overcome this problem one needs to define some new transformation with components $\widehat{\mathcal{Q}}^0_{j,s,k}, \widehat{\mathcal{Q}}^1_{j,s,k}$, that are related to the previous ones as

$$\widehat{\mathcal{Q}}^{\phi}_{j,s,k} = \mathcal{Q}^{\phi}_{j,s,k} - \frac{\Psi_{j,0}}{N_j} \mathcal{Q}^{\phi}_{j,s,k} \Psi^*_{j,0}. \tag{19}$$

The elements of this transformation, these new Bogoliubov operators, are expressed in terms of the Bogoliubov wave functions of our system $f_{j,s,k}$, $\widetilde{f}_{j,s,k}$ as

$$\widehat{\mathcal{Q}}^{\phi}_{j,s,k} = \frac{f_{j,s,k} + (-1)^{\phi} \widetilde{f}_{j,s,k}}{2}, \tag{20}$$

where

$$\begin{aligned}
f_{1,-,k} = f_{2,-,k} &= \left[\frac{\epsilon_k}{2E_{-,k}}\right]^{1/2}, \\
\widetilde{f}_{1,-,k} = \widetilde{f}_{2,-,k} &= \left[\frac{E_{-,k}}{2\epsilon_k}\right]^{1/2}, \\
f_{1,+,k} = f_{2,+,k} &= \left[\frac{\epsilon_k + \hbar\Omega}{2E_{+,k}}\right]^{1/2}, \\
\widetilde{f}_{1,+,k} = \widetilde{f}_{2,+,k} &= \left[\frac{E_{+,k}}{2\left(\epsilon_k + \hbar\Omega\right)}\right]^{1/2}.
\end{aligned}$$

The spin mode branch is gapped while the density mode branch is gapless. For the latter, at low values of the momentum k the dispersion is linear, with a speed of sound $c_d = \sqrt{n\left(g + g_{12}\right)/(2m_{\mathrm{B}})}$. On the contrary for the gapped branch, the dispersion relation goes as k^2 for low k, and at $k = 0$, it has a gap

$$E_{\mathrm{gap}} = \sqrt{2\hbar\Omega\left[\left(g - g_{12}\right)n + 2\hbar\Omega\right]}. \tag{21}$$

This corresponds to the Josephson frequency for small amplitude oscillations. As we will see the fact that there are two branches in the spectrum will give rise to two different noise sources.

Furthermore, one should note that, had we not introduced the Rabi coupling term in the Hamiltonian, the latter would commute with both n_1 and n_2 such that we would have two broken continuous symmetries and both branches would be gapless (notice that $E_{\mathrm{gap}} \to 0$ when $\hbar\Omega \to 0$). In this case, the low momentum excitations would be both phase-like, as it has to be for Goldstone modes of the $U(1)$x$U(1)$ broken symmetries [57]. Hence the introduction of the Rabi coupling term, results in the system having only one continuous broken symmetry, namely only n has to be conserved now and not both n_1 and n_2. The long wavelength limit of the Goldstone mode corresponds to a low-amplitude phonon fluctuation in which the total density oscillates and the unlike atoms move in unison (i.e., with the same superfluid velocity). In contrast, in the long wavelength gap mode the unlike atoms move in opposite directions, while their center of mass remains at rest. This fluctuation is then reminiscent of the motion of ions in an optical phonon mode, which also exhibits a gapped dispersion. At zero momentum, the gap mode corresponds to an infinitesimal Josephson-like oscillation of the populations in the distinguishable internal states. In the strong Josephson coupling regime we have closed orbits around a fixed point for the Josephson Hamiltonian, with vanishing mean polarisation (or population imbalance) and a phase difference around π if $\hbar\Omega \geq 0$, giving rise to plasma-like oscillations.

2.2 Transformed Impurity-Bath interaction

In terms of the original annihilation and creation operators, the impurity-bath term reads as

$$\begin{aligned}
H_{\mathrm{IB}} &= \sum_j \frac{1}{V} \sum_{k,q} V^{(j)}_{\mathrm{IB}}(k)\, \rho_{\mathrm{I}}(q)\, a^{\dagger}_{j,k-q} a_{j,k} \\
&= \sum_j \sqrt{\frac{n_j}{V}} \sum_{k\neq 0} \rho_{\mathrm{I}}(k)\, V^{(j)}_{\mathrm{IB}} \left(a_{j,k} + a^{\dagger}_{j,-k}\right),
\end{aligned} \tag{22}$$

with $\rho_I(q) = \int_{-\infty}^{\infty} e^{-iqx'} \delta(x' - x)\, dx'$, $V^{(j)}_{\mathrm{IB}}(k) = \mathcal{F}_k[g^{(j)}_{\mathrm{IB}} \delta(x - x')]$ where $\mathcal{F}$ is the Fourier trasnform. Furthermore, n_j, with $j = 1, 2$, is the averaged density of the j^{th} bath. The second line of Eq. (22) is a consequence of the assumption that the bosons condense. We will consider two cases for the coupling of the impurity to the baths.

1. In the first scenario the impurity couples to the two baths in the same way

$$g^{(1)}_{\mathrm{IB}} = g^{(2)}_{\mathrm{IB}} = g_{\mathrm{IB}}, \tag{23}$$

2. while in the second scenario, the interactions are attractive with one of the baths and repulsive with the other the other,

$$g^{(1)}_{\mathrm{IB}} = -g^{(2)}_{\mathrm{IB}} = g_{\mathrm{IB}}. \tag{24}$$

After the Bogoliubov transformation the impurity-bath term reads in both cases as

$$1.\ H^{(-)}_{IB} = \left[\frac{n}{V}\right]^{\frac{1}{2}} \sum_{j,k\neq 0} \rho_I(k)\, g_{\mathrm{IB}} \left[\widehat{\mathcal{Q}}^0_{j,-,k} + \widehat{\mathcal{Q}}^1_{j,-,k}\right] x_{-,k},$$

$$2.\ H^{(+)}_{IB} = \left[\frac{n}{V}\right]^{\frac{1}{2}} \sum_{j,k\neq 0} \rho_I(k)\, g_{\mathrm{IB}} \left[\widehat{\mathcal{Q}}^0_{j,+,k} + \widehat{\mathcal{Q}}^1_{j,+,k}\right] x_{+,k},$$

where $x_{\pm,k} := \left(b_{\pm,k} + b^{\dagger}_{\pm,k}\right)$. These equations show that in case 1 the impurity only couples to the density $(-)$ mode of the bosonic baths, while in case 2 it

couples only to the spin (+) mode. For both cases, we rewrite the impurity-bath terms as

$$H_{\mathrm{IB}}^{s}=\sum_{\substack{j,k\neq 0\\ s\in\{+,-\}}} V_{j,s,k}e^{ikx}\left(b_{s,k}+b_{s,-k}^{\dagger}\right), \tag{25}$$

where $s=-$ for case 1 and $s=+$ for case 2, and

$$V_{j,s,k}=\sqrt{\frac{n}{V}}g_{\mathrm{IB}}\left(\widehat{\mathcal{Q}}_{j,s,k}^{0}+\widehat{\mathcal{Q}}_{j,s,k}^{1}\right). \tag{26}$$

We note here that $\widehat{\mathcal{Q}}_{1,s,k}^{0}+\widehat{\mathcal{Q}}_{1,s,k}^{1}=\widehat{\mathcal{Q}}_{2,s,k}^{0}+\widehat{\mathcal{Q}}_{2,s,k}^{1}$, such that $V_{1,s,k}=V_{2,s,k}=\widehat{V}_{s,k}$. We linearize the interaction (see [35] for validity of this assumption) to get

$$H_{\mathrm{IB}}=\sum_{\substack{k\neq 0\\ s\in\{+,-\}}} V_{s,k}\left(\mathbb{I}+ikx\right)\left(b_{s,k}+b_{s,-k}^{\dagger}\right). \tag{27}$$

where $V_{s,k}=2\widehat{V}_{s,k}$. Thus, after a redefinition $b_{s,k}\rightarrow b_{s,k}-\frac{V_{s,k}}{E_{s,k}}\mathbb{I}$, the final total Hamiltonian reads as

$$H=H_{\mathrm{I}}+\sum_{\substack{k\neq 0\\ s\in\{+,-\}}} E_{s,k}b_{s,k}^{\dagger}b_{s,k}+\sum_{\substack{k\neq 0\\ s\in\{+,-\}}}\hbar g_{s,k}\pi_{s,k}, \tag{28}$$

with $g_{j,s,k}=kV_{s,k}/\hbar$ and $\pi_{s,k}=i\left(b_{k,s}-b_{k,s}^{\dagger}\right)$ the momentum of the bath particles. We see that as in [35], the coupling occurs between the position of the impurity and the momentum of the bath particles. However, in our work, the coupling can take place to one of the two different quasiparticle branches, depending on the form of the impurity-baths interactions.

3 Spectral densities

The spectral densities can be obtained from the self-correlation functions [35] for each environment (corresponding to cases 1 and 2). These read

$$\mathcal{C}\left(t\right)=\sum_{\substack{k\neq 0\\ s\in\{+,-\}}}\hbar g_{s,k}^{2}\left\langle\pi_{s,k}\left(t\right)\pi_{s,k}\left(0\right)\right\rangle/\hbar. \tag{29}$$

Using that the bath is composed of bosons for which

$$\left\langle b_{k,s}^{\dagger}b_{k,s}\right\rangle=\frac{1}{e^{\frac{\hbar\omega_{k}}{k_{B}T}}-1}, \tag{30}$$

we obtain

$$\begin{aligned}\mathcal{C}\left(t\right)&=\sum_{\substack{k\neq 0\\ s\in\{+,-\}}} g_{s,k}^{2}\left[\coth\left(\frac{\hbar\omega_{k}}{2k_{B}T}\right)\cos\left(\omega_{k}t\right)-i\sin\left(\omega_{k}t\right)\right]\\&=\nu\left(t\right)-i\lambda\left(t\right),\end{aligned} \tag{31}$$

where

$$\begin{aligned}\nu\left(t\right)&=\int_{0}^{\infty}\sum_{s\in\{+,-\}}J^{D}\left(\omega\right)\coth\left(\frac{\hbar\omega}{2k_{B}T}\right)\cos\left(\omega t\right)d\omega,\\ \lambda\left(t\right)&=\int_{0}^{\infty}\sum_{s\in\{+,-\}}J^{D}\left(\omega\right)\sin\left(\omega t\right)d\omega.\end{aligned} \tag{32}$$

In these definitions we used the spectral density,

$$J^{D}\left(\omega\right)=\hbar\sum_{k\neq 0}\left(g_{s,k}\right)^{2}\delta\left(\omega-\omega_{k}\right). \tag{33}$$

The spectral density is then evaluated in the continuous frequency limit as

$$\begin{aligned}&J^{D}\left(\omega\right)=\\&4ng_{\mathrm{IB}}^{2}\frac{D_{d}}{\hbar\left(2\pi\right)^{d}}\int dkk^{d+1}\left(\mathcal{U}_{s,k}+\mathcal{V}_{s,k}\right)^{2}\frac{\delta\left(k-k_{E_{s}}(\omega)\right)}{\partial_{k}E_{s}(k)\left|_{k=k_{E_{s}}(\omega)}\right.},\end{aligned} \tag{34}$$

where D_d is the surface of the hypersphere in the momentum space with radius k in d-dimensions. In the particular case of 1D becomes $D_1=2$.

To obtain the expression for the continuous frequency case, the inverse of the dispersion relation from Eq. (9) is needed. For this general energy spectrum, obtaining such inverse function is not easy. However this is indeed possible for the simplified case, Eqs. (16)–(17). The inverse of the density (-) branch which is the one to which the impurity couples for the case 1 type of coupling, reads

$$\begin{aligned}&k_{E_{-}}\left(\omega\right)=\\&\sqrt{m_{\mathrm{B}}ng}\left[\frac{g_{12}}{g}-1+\sqrt{1-\frac{2g_{12}}{g}+\left[\frac{g_{12}}{g}\right]^{2}+\left[\frac{2\omega}{ng}\right]^{2}}\right]^{\frac{1}{2}}.\end{aligned} \tag{35}$$

With this, for the density (−) branch (case 1 type of coupling), the spectral density is

$$J_{-}\left(\omega\right)=\tilde{\tau}_{-}\frac{G_{-}(\omega)^{3/2}}{\sqrt{F_{-}(\omega)}}, \tag{36}$$

with

$$F_{-}(\omega)=1+\left(\frac{\omega}{\Lambda_{-}}\right)^{2}, \tag{37}$$

$$G_{-}(\omega)=-1+\sqrt{F_{-}(\omega)}, \tag{38}$$

$$\tilde{\tau}_{-}=\frac{\left(2g_{\mathrm{IB}}\right)^{2}nm_{\mathrm{B}}^{3/2}}{2^{1/2}\pi}\sqrt{\Lambda_{-}}, \tag{39}$$

and where $\Lambda_{-}=n\left(g+g_{12}\right)/2\hbar$ is the cutoff frequency, which resembles the one in [35] when g is replaced by $\frac{g+g_{12}}{2}$. In the limit of $\omega\ll\Lambda_{-}$, the spectral density can be simplified to

$$J_{-}\left(\omega\right)=m_{I}\tau_{-}\omega^{3}, \tag{40}$$

where

$$\tau_{-}=\frac{\left(2\eta\right)^{2}}{2\pi m_{I}}\left(\frac{m_{\mathrm{B}}}{n\left(g+g_{12}\right)^{1/3}}\right)^{3/2}, \tag{41}$$

with $\eta_- = \frac{g_{\rm IB}}{g+g_{12}}$. Thus, for the the π-state equilibrium configuration one obtains a cubic spectral density.

3.1 Spin branch coupling

For the spin (+) branch (case 2 type of coupling), the inverse of the spectrum reads as

$$k_{E_+}(\omega) = \sqrt{m_{\rm B} n g}\times \tag{42}$$
$$\left[\frac{g_{12}}{g} - 1 - \frac{4\hbar\Omega}{ng} + \sqrt{1 - \frac{2g_{12}}{g} + \left[\frac{g_{12}}{g}\right]^2 + \left[\frac{2\omega}{ng}\right]^2}\right]^{\frac{1}{2}}.$$

In this case, the spectral density is

$$J_+(\omega) = m_I \widetilde{\tau}_+ \frac{G_+(\omega)}{\sqrt{F_+(\omega)}}, \tag{43}$$

where

$$F_+(\omega) = 1 + \left(\frac{\omega}{\Lambda_+}\right)^2,$$
$$G_+(\omega) = W(\omega)\left[W(\omega) + \frac{1}{2} - \frac{1}{2}\sqrt{1 + \left[\frac{E_{\rm gap}}{\Lambda_+}\right]^2}\right]^{\frac{1}{2}},$$
$$W(\omega) = -\frac{1}{2} + \sqrt{F_+(\omega)} - \frac{1}{2}\sqrt{1 + \left[\frac{E_{\rm gap}}{\Lambda_+}\right]^2},$$
$$\widetilde{\tau}_+ = \frac{(2g_{\rm IB})^2 n m_{\rm B}^{3/2}}{2^{1/2}\pi m_I}\sqrt{\Lambda_+}, \tag{44}$$

with $\Lambda_+ = n(g - g_{12})/2\hbar$. We note that to interpret $\widetilde{\tau}_+$ as a relaxation time, as is custom to do (see [35]), one has to impose $g \geq g_{12}$ to assure it remains a real quantity. In other case, the spectral density will be imaginary (note $\frac{G_+(\omega)}{\sqrt{F_+(\omega)}}$ is independent of the sign of $g - g_{12}$).

Let us find how the spectral density in Eq. (43) simplifies in two limiting cases. First, in the absence of coherent coupling, $\Omega = 0$, the gap vanishes, $E_{\rm gap} = 0$. In this case, Eq. (43) is equal to that of the density mode, upon the interchange $\Lambda_- \to \Lambda_+$. Therefore, on the long time limit $\omega \ll \Lambda_+$ we obtain the same cubic behavior of the spectral density. We illustrate this case in Fig. 2. In panel (a) we show that the two branches of the energy spectra have the same behavior, that is, linear at low k and parabolic for large k.

Second, we consider the case of finite Ω which implies $E_{\rm gap} > 0$. A requirement which we impose on the spectral density is that one cannot consider frequencies lower than the gap energy $E_{\rm gap}$. Physically, one can interpret this as follows: Since the energy spectrum of the bath is gapped, with a gap given by Eq. (21), the spectral density cannot assign a weight at frequencies lower than this, because the bath cannot excite the impurity with such frequencies since it is not part of its spectrum. Then, we simplify the spectral density as

$$\widehat{J}_+(\omega) = \Theta(\omega - E_{\rm gap}) J_+(\omega), \tag{45}$$

with $\Theta(.)$ the step delta function.

Let us now comment on the frequency region right above the energy gap of our system. To this end, we replace $\omega = E_{\rm gap} + \epsilon$, where $\epsilon > 0$. We use ϵ as the small value expansion parameter in our case, i.e. we consider the limit $\epsilon \ll E_{\rm gap}$, such that $\omega \approx E_{\rm gap}$. We furthermore introduce a cutoff Λ, for which it holds that $\epsilon \ll \Lambda - E_{\rm gap}$. The expressions in the spectral density will now read as

$$F_+(\epsilon) = 1 + \left(\frac{E_{\rm gap}}{\Lambda_+}\right)^2, \tag{46}$$
$$W(\epsilon) = -\frac{1}{2} + \frac{1}{2}\sqrt{1 + \left(\frac{E_{\rm gap}}{\Lambda_+}\right)^2} + \frac{E_{\rm gap}}{\Lambda_+}\left(E_{\rm gap}^2 + \Lambda_+^2\right)^{-\frac{1}{2}}\epsilon,$$

such that

$$G_+(\epsilon) = \tag{47}$$
$$\left[-\frac{1}{2} + \frac{1}{2}\sqrt{1 + \left[\frac{E_{\rm gap}}{\Lambda_+}\right]^2}\right]\left[\frac{E_{\rm gap}}{\Lambda_+}\right]^{\frac{1}{2}}\left[E_{\rm gap}^2 + \Lambda_+^2\right]^{-\frac{1}{4}}\epsilon^{\frac{1}{2}}.$$

Hence the spectral density is

$$\widehat{J}_+(\epsilon) = \Theta(\epsilon)\tau_+\epsilon^{1/2}, \tag{48}$$

with

$$\tau_+ = \widetilde{\tau}_+ \frac{\left(-\frac{1}{2} + \frac{1}{2}\sqrt{1 + \left(\frac{E_{\rm gap}}{\Lambda_+}\right)^2}\right)(E_{\rm gap})^{\frac{1}{2}}}{\left(1 + \left(\frac{E_{\rm gap}}{\Lambda_+}\right)^2\right)^{1/4}}. \tag{49}$$

The final form of the spectral density, after introducing a cutoff Λ, to avoid the related ultraviolet divergencies mentioned above, is

$$\widehat{J}_+(\omega) = \tag{50}$$
$$\Theta(\omega - E_{\rm gap})\tau_+[\omega - E_{\rm gap}]^{\frac{1}{2}}\Theta(\Lambda + E_{\rm gap} - \omega).$$

We introduced a hard cutoff to our spectral density as this better describes the physical system we study. Such a spectral density, i.e. with an exponent on the frequencies less than 1, is often associated to subdiffusive impurity dynamics. Note that in the results that we present below, we assume $g \approx g_{12}$ as in [58], which significantly simplifies the expression for the coefficient of the spectral density τ_+ without changing its behavior. In particular in this case $\tau_+ = (2g_{\rm IB})^2 n m_{\rm B}^{3/2}/2^{1/2}\pi m_I$. In Fig. 2(b), we show how the approximate spectral density in Eq. (50), under the assumption $\epsilon \ll E_{\rm gap}$, compares to the

original spectral density. For vanishingly small values of $E_{\rm gap}$ the spectral density approaches the form of that of the density mode, i.e. it goes as $\propto \omega^3$, as expected. In the limit we are interested, that is, for finite $E_{\rm gap}$, the spectral density behaves approximately as in Eq. (50) (see inset in Fig. 2(b)).

Such gapped spectral densities as in Eq. (50), have been studied extensively in the literature. In general, they are usually related to semiconductors [59–61] or photonic crystals (PC) [62]. In particular, the simplified form of the spectral density, Eq. (50), is related in particular with 3D PCs. The latter, are artificial materials engineered with periodic dielectric structures [63]. If one considers an atom embedded in such a material, it is known that if the resonant frequency of the excited atom approaches the band gap edge of the PC, strong localization of light, atom-photon bound states, inhibition of spontaneous emission and fractionalized steady-state inversion appear [64–67]. The rapidly varying distribution of field modes near the band gap [62, 68] requires a non-Markovian description [69] of the reduced dynamics of quantum systems coupled to the radiation field of a PC [66, 67, 70–72]. This enhanced appearance of non-Markovian effects is also confirmed by a recent study based on exact diagonalization [73]. In this study it was observed that for frequencies of the bath much larger than the band gap, energy transfer between the system and the bath is such that information and energy flow irreversibly from system to bath leading to Markovian dynamics. Conversely, at the edges of the gaps, one observes the largest backflow of information where the energy bounces between the system and bath leading to non-Markovian evolution of the system. Furthermore, deep within the band gap, less excitations and energy are exchanged between the system and the bath, which is shown to lead to localized modes [74], expressed as dissipationless oscillatory behavior, plus non-exponential decays (such as for example fractional relaxations [75]).

From the work in [74], a relationship is suggested of such long-lived oscillations that appear in the dynamics of a system coupled to a bath with a gapped spectral density, with the fact that the Hamiltonian of the system might have thermodynamic and dynamic instabilities. This is the case when the Hamiltonian is unbounded from below, i.e. non-positive. Physically this happens when one deals with Hamiltonians that do not conserve the particles number, and this is indeed the case for the Hamiltonian of the free quantum Brownian motion we study here. Hence, as a result, this unbounded Hamiltonian induces dynamical instabilities in the long-time regime, corresponding to the limit $\omega \ll \Lambda$. In practice, as in the spirit of [35], one can show that the effect of the bath on the impurity is not only to dissipate its energy, but as well to introduce an inverse parabolic potential in which the impurity is diffusing (which would work as a renormalization of the trapping frequency had we considered a harmonic trapping potential). This inverse parabolic potential is understood to be a consequence of the unboundedness of the Hamiltonian, and is what is resulting in the dynamical instability of the long time solution of the impurity dynamics. Unfortunately, contrary to the case in [35], we will not consider a harmonic trap for the impurity, and hence the positivity of the Hamiltonian is violated irrespective of the strength of the coupling of the impurity to the bath. In practice one would study the impurity constrained in a box of a certain size, which if included in the modelling of the system, would result in a positively defined Hamiltonian, at the price of complicating significantly the analytical solution for the impurity's dynamics. Hence, we assume here that we are looking at timescales where the effect of the finite sized box are not manifested. Theoretically, there are also a number of other ways to circumvent this problem, even without referring to the presence of a box, such as taking into account bilinear terms in the impurity's or bath's operators in the Hamiltonian as in [76–79]. In any case, we will show below that for the regime of the transient effect that we are interested in, this will not change our results.

Following the approach sketched above, we take advantage of the simplicity of the Fröhlich like Hamiltonian we are considering above. Furthermore, we remind that we will look at the long time dynamics of the impurity, i.e. $\omega \ll \Lambda$, as was implied by the above study on the spectral density's form. In addition, one should take into account the dissipationless oscillatory behavior, which can also be expressed as an incomplete decay of the Green function impurity propagator which we will study below. In fact by identifying the equivalence of the appearance of these oscillations with the incomplete decay of the Green function, this provides us with a very simple condition upon which the long-lived oscillations appear, that is that the Green function has at least one purely imaginary pole, which can be shown to only be possible for frequencies within the band gap [62]. We will study this in the next section.

4 Heisenberg equations and their solution

In this section, we derive the equation of motion for the impurity, which will allow us to study its diffusive behavior under various scenarios. To do so, we begin with the Heisenberg equations of motion for both the impurity and the bath particles. The latter set of equations can be solved, and we use this solution to obtain a Langevin like equation of motion for the impurity. The Heisenberg equations for the bath par-

ticles are

$$\frac{db_{s,k}(t)}{dt} = i\left[H, b_{s,k}(t)\right] = -i\Omega_{s,k} b_{s,k}(t) - \hbar\sum_{j=1}^{2} g_{s,k}^{(j)} x(t),$$

$$\frac{db_{s,k}^{\dagger}(t)}{dt} = \frac{i}{\hbar}\left[H, b_{s,k}^{\dagger}(t)\right] = \frac{i}{\hbar}\Omega_{s,k} b_{s,k}^{\dagger}(t) - \hbar\sum_{j=1}^{2} g_{s,k}^{(j)} x(t), \quad (51)$$

and for the central particle

$$\frac{dx(t)}{dt} = \frac{i}{\hbar}\left[H, x(t)\right] = \frac{p(t)}{m_I}, \quad (52)$$

$$\frac{dp(t)}{dt} = \frac{i}{\hbar}\left[H, p(t)\right] = \frac{i}{\hbar}\left[U(x), x(t)\right] - \sum_{\substack{k\neq 0 \\ j=\{1,2\} \\ s=\{+,-\}}} \hbar g_{s,k}^{(j)} \pi_{s,k}(t).$$

Substituting the solutions of the equations of motion for the bath into that of the central particle, one gets

$$\ddot{x}(t) + \frac{\partial}{\partial t}\int \Gamma(t-s)\, x(s)\, ds = \frac{B(t)}{m_I}, \quad (53)$$

where

$$\Gamma(\tau) = \frac{1}{m_I}\int_0^{\infty} \frac{\sum_{\substack{j=\{1,2\} \\ s=\{+,-\}}} J_s^{(j)}(\omega)}{\omega} \cos(\omega\tau)\, d\omega,$$

$$B(t) = \sum_{k\neq 0}\sum_{\substack{j=\{1,2\} \\ s=\{+,-\}}} i\hbar\, g_{s,k}^{(j)}\left(b_{s,k}^{\dagger}(t)\, e^{i\omega_k t} - b_{s,k}(t)\, e^{-i\omega_k t}\right), \quad (54)$$

are the damping and noise terms, respectively. Note that in Eq. (53) we neglected a term $-\Gamma(0)\, x(t)$. This term may introduce dynamic instabilities in our system in the long time regime. As in [35], we neglect it as these instabilities are unphysical, that is, will not occur in a physical realization of the system and will only occur in the long time behavior. To be more specific, for the coupling to the density mode this term reads as,

$$\Gamma_-(0) = \tau_- \frac{\Lambda_-^3}{3}. \quad (55)$$

For the coupling to the spin mode this term reads as

$$\Gamma_+(0) = \tau_+\left[-\pi E_{Gap}^{1/2} + 2\left(\Lambda + E_{Gap}\right)^{0.5} \times F_{2,1}\left(-\frac{1}{2}, -\frac{1}{2}; \frac{1}{2}; \frac{E_{Gap}}{\Lambda + E_{Gap}}\right)\right]. \quad (56)$$

As in [35], the solution of Eq. (53) takes the form

$$x(t) = G_1(t)x(0) + G_2(t)\dot{x}(0) + \frac{1}{m_I}\int_0^t G_2(t-s)B(s)ds, \quad (57)$$

with the corresponding Green functions given by

$$\mathcal{L}_z\left[G_1(t)\right] = \frac{z}{z^2 + z\mathcal{L}_z\left[\Gamma(t)\right]} = \frac{1}{z + \mathcal{L}_z\left[\Gamma(t)\right]}, \quad (58)$$

$$\mathcal{L}_z\left[G_2(t)\right] = \frac{1}{z^2 + z\mathcal{L}_z\left[\Gamma(t)\right]}, \quad (59)$$

where $\mathcal{L}_z[\cdot]$ represents the Laplace transform. The expressions for $G_1(t)$ and $G_2(t)$ depend on the specific type of bath we consider. For the first scenario (coupling to the density mode), in [35] it was found that $\Gamma(t)$ is

$$\Gamma_-(t) = \frac{\tau_-}{t^3}\left[2\Lambda_- t\cos(\Lambda t) - 2\left(2 - \Lambda_-^2 t^2\right)\sin(\Lambda_- t)\right], \quad (60)$$

and under the assumption of $z \ll \Lambda_-$

$$\mathcal{L}_z\left[\Gamma_-(t)\right] = \tau_-\Lambda_- z + \mathcal{O}\left(z^2\right), \quad (61)$$

which results in

$$\mathcal{L}_z\left[G_1(t)\right] = \frac{1}{\left(1 + \Lambda_-\tau_-\right)z}, \quad (62)$$

and

$$\mathcal{L}_z\left[G_2(t)\right] = \frac{1}{\left(1 + \Lambda_-\tau_-\right)z^2}. \quad (63)$$

Then, one obtains

$$G_1(t) = \frac{1}{\left(1 + \Lambda_-\tau_-\right)}, \quad (64)$$

and

$$G_2(t) = \frac{t}{\left(1 + \Lambda_-\tau_-\right)}, \quad (65)$$

where we see that the Green functions has an identical form to that of [35]. More importantly, $G_2(t)$ diverges at $t \to \infty$, a consequence of the fact that an equilibrium state is not reached at this limit, as we see in next section.

For the second case (coupling to the spin mode), as discussed in previous section the spectral density is gapped and given by Eq. (50). To proceed, we first need an expression for the Laplace transform $\mathcal{L}_z\left[\Gamma_+(t)\right]$ which can be shown to read as

$$\mathcal{L}_z\left[\Gamma_+(t)\right] = \int_0^{\infty}\left[\int_0^{\infty} d\omega \frac{\widehat{J}_+(\omega)}{\omega}\cos(\omega t)\right] e^{-zt} dt$$
$$= z\int_0^{\infty} d\omega \frac{\widehat{J}_+(\omega)}{\omega\left(\omega^2 + z^2\right)} = \frac{\tau_+}{z\left(E_{gap}^3 + E_{gap} z^2\right)}\Lambda^{1.5}$$
$$\times\left[-\frac{E_{\rm gap}}{3}(E_{\rm gap} + iz)F_{2,1}\left(1, \frac{3}{2}; \frac{5}{2}; -\frac{\Lambda}{E_{\rm gap} - iz}\right)\right.$$
$$-\frac{E_{\rm gap}}{3}\left(E_{\rm gap} - iz\right)F_{2,1}\left(1, \frac{3}{2}; \frac{5}{2}; -\frac{\Lambda}{E_{\rm gap} + iz}\right)$$
$$\left.+\frac{2}{3}\left(E_{\rm gap}^2 + z^2\right)F_{2,1}\left(1, \frac{3}{2}; \frac{5}{2}; -\frac{\Lambda}{E_{\rm gap}}\right)\right], \quad (66)$$

where $F_{2,1}(\alpha,\beta;\gamma;z)$ is the hypergeometric function

$$F_{2,1}(\alpha,\beta;\gamma;z)=\sum_{n=0}^{\infty}\frac{(\alpha)_n(\beta)_n}{(\gamma)_n}\frac{z^n}{n!}, \tag{67}$$

with $(\cdot)_n$ being the Pochhammer symbol. Unfortunately, to invert the Laplace transform in Eq. (59), given Eq. (66), is rather complicated. For this reason we restrain ourselves to study only the long-time limit, determined by $z \ll \Lambda$. In this case the inverse Laplace transform of the Green's function in Eq. (59), reads as

$$\begin{aligned} &G_2(t)=At, \qquad (68)\\ &A=E_{\rm gap}^5\Big[E_{\rm gap}^5+\frac{2}{3}E_{\rm gap}^2\Lambda^{1.5}\tau_+F_{2,1}\left(1,\frac{3}{2};\frac{5}{2};\frac{-\Lambda}{E_{\rm gap}}\right)\\ &-\frac{4}{5}E_{\rm gap}\Lambda^{2.5}\tau_+F_{2,1}\left(2,\frac{5}{2};\frac{7}{2};-\frac{\Lambda}{E_{\rm gap}}\right)\\ &+0.285714\Lambda^{3.5}\tau_+F_{2,1}\left(3,\frac{7}{2};\frac{9}{2};-\frac{\Lambda}{E_{\rm gap}}\right)\Big]^{-1}, \end{aligned}$$

which has the same time dependence as in case 1 (coupling to the density mode). We also find $G_1(t)=A$ which is again a constant and hence does not play a role in the time dependence of the MSD which we are interested in. Unfortunately this is as far as we can get analytically, as contrary to the coupling to the density mode, even though we have the Green function at hand, using it to obtain an analytic expression for the MSD of the impurity which is our ultimate goal is not possible.

Equation (65) as well as Eq. (66) have been both obtained at the long time limit, which implied expanding the Laplace transform of the damping kernel $\mathcal{L}_z[\Gamma_-(t)],\mathcal{L}_z[\Gamma_+(t)]$ at the first order in $z/\Lambda_-, z/\Lambda$. In general, one could have considered higher orders of the aforementioned expansion, but should then be careful in inverting the Laplace transform to obtain the Green function in defining the relevant Bromwich integral in the complex plane in such a way as to not include the roots which correspond to divergent runaway solutions [35]. Even if one would do so, the result for the Green function would not change much, and this can be proven by considering a numerical inversion of the Laplace transform for the Green function, where the long time limit assumption is not made. For the coupling to the density mode this was shown using the Zakian method in [35]. For the spin mode, we checked this using the same method. Moreover, we contrasted its results to two other methods for numerically inverting a Laplace transform, in particular, the Fourier and the Stehfest methods [80]. The Zakian method, gives the inverse of the Laplace transform of a function $F(z)$ in the following form

$$f(t)=\frac{2}{t}\sum_{j=1}^{N}Re\left[k_jF\left(\frac{\beta_j}{t}\right)\right], \tag{69}$$

where k_j and β_j are real and complex constants given in [80]. With all of these methods, the Green function behaves linearly with time for the range of parameters we considered. In fact in the numerical results presented in the next section, the Zakian method was used to obtain the Green function, such that our results are not restricted just to the long time limit, $z \ll \Lambda$.

In addition, we are also now in a position to check the presence of the long-lived oscillations in our system. As was mentioned before, this can only be the case if the Green function exhibits a purely imaginary pole, which if it exists, should correspond to a frequency within the bandgap. As is shown in [81], this will be the case, for the frequency that is a solution of

$$\omega^2+\Gamma(0)-\Delta(\omega)=0, \tag{70}$$

where

$$\begin{aligned}\Delta(\omega)&:=P\int_0^{\infty}\frac{\widehat{J}_+(\omega')}{\omega-\omega'}d\omega'\\ &=-\frac{2\tau_+\Lambda^{1.5}F_{2,1}\left(1,\frac{3}{2};\frac{5}{2};-\frac{\Lambda}{E_{\rm gap}-\omega}\right)}{3(E_{\rm gap}-\omega)}, \end{aligned}\tag{71}$$

is the bath self energy correction, where P denotes the principal value. One can show that the expression of Eq. (71) is always non-positive for $\omega < E_{\rm gap}$ and hence the condition in Eq. (70) is never satisfied, such that we do not have to worry about these oscillations in the transient dynamics that we will study in the next section.

Finally, one can evaluate the validity of the linearity assumption which allowed us to consider a linear coupling between the BEC and the impurity (see Hamiltonian in Eq. (27)) in terms of the physical parameters of the system. This assumption reads as $kx \ll 1$. In [35] it was shown that, as a function of the temperature, there exist a maximum time for which the linear assumption holds. In the system discussed here, since an expression for the MSD cannot be found, for each set of parameters one has to evaluate numerically the long-time behavior of the MDS and determine the maximum time for which the assumption holds. To this end, one has to note that, differently to [35], for the coupling to the spin mode the momenta grows parabolically with ω even for small k and there is an energy gap. Then, to evaluate the criteria ($kx \ll 1$), one has to use the expression for the energy, Eq. (17) together with the numerically evaluated MSD. We checked this condition in the numerical examples presented in next section. A final comment is that, we also made sure that the assumption of a purely 1D BEC was valid, by checking that the spatial extend of the motion did not exceed the phase coherence length [52].

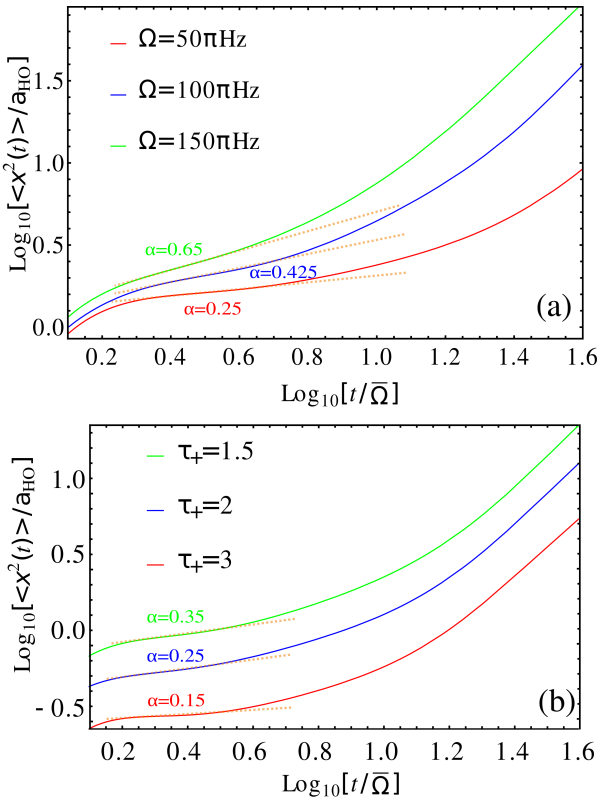

Figure 3: Mean square displacement *vs* time for the case of coupling to the spin mode. A cutoff of $\Lambda = 10\bar{\Omega}$ was used, where $\bar{\Omega} = 1000\pi Hz$. In (a) we plot it for different coherent couplings Ω and in (b) for different couplings to the bath. The MSD shows three regimes, where it behaves approximately as $\mathrm{MSD}(t) \propto t^{\alpha}$, and therefore linearly in log-log pots, with a different slope given by the anomalous exponent α: (i) an initial short time behavior, where $\alpha \approx 2$; (ii) a nontrivial transient subdiffusive behavior, where $\alpha < 1$. We plot a dashed orange line as a guide to the eye, to illustrate the different slopes in this regime; (iii) a long time ballistic regime, with $\alpha = 2$. In (a) we show that, as Ω is reduced, the subdiffusive platteau enlarges and α gets smaller. In (b) we show that increasing the couplings to the bath τ_+, also enlarges the plateau and reduces α. We consider Rb and K atoms for BEC and impurities, respectively. We use $g = g_{12} = 2.15 \times 10^{-37} J \cdot m$, density $n = 7(\mu m)^{-1}$, and impurity-BEC $g_{\mathrm{IB}} = 0.5 \times 10^{-37} J \cdot m$; We take $\tau_+ = 1$ in (a) and $\Omega = 100\pi Hz$ in (b). The BEC was assumed to be in the low temperature regime, i.e. when $\coth\left(\frac{\hbar\omega}{2k_BT}\right) \to 1$ holds.

5 Results: Mean square displacement

With the Green propagator and the spectral density at hand, we are now in a position to evaluate the MSD. This, as shown in [35], is evaluated in the long time limit $\omega \ll \Lambda_-, \Lambda$ as

$$\begin{aligned}\left\langle [x(t) - x(0)]^2 \right\rangle &= \mathrm{MSD}(t) = G_2^2(t)\langle \dot{x}^2(0)\rangle \\ &+ \frac{1}{2}\int_0^t ds \int_0^t d\sigma G_2(s) G_2(\sigma) \left\langle \{B(s), B(\sigma)\} \right\rangle_{\rho_B}, \end{aligned} \tag{72}$$

where we assumed that the impurity-bath are initially in a product state $\rho(0) = \rho_B \otimes \rho_S(0)$, where ρ_B is the thermal Gibbs state for the bath at temperature T. The initial conditions of the impurity and bath oscillators are then uncorrelated. Then, averages of the form $\langle \dot{x}(0) B(s)\rangle$ vanish. To treat the second term in Eq. (72), we note that

$$\left\langle \{B(s), B(\sigma)\} \right\rangle_{\rho_B} = 2\hbar\nu(s-\sigma), \tag{73}$$

where $\nu(t)$ is defined as in Eq. (32).

In case 1 (coupling to density mode) the spectral density reads as in Eq. (40). Then, the MSD behaves the same way as in [35], with the only difference of replacing $g \to g + g_{12}$. Hence the impurity will again superdiffuse as

$$\left\langle [x(t) - x(0)]^2 \right\rangle = \left[\langle \dot{x}^2(0)\rangle + \frac{\tau_- \Lambda_-^2}{2} \right] \left(\frac{t}{\zeta}\right)^2, \tag{74}$$

where $\zeta = 1 + \tau_- \Lambda_-$. Note that the superdiffusive behavior $\langle x^2(t)\rangle \propto t^2$ appears for both low temperature ($\coth(\hbar\omega/2k_BT) \approx 1$) and high temperature ($\coth(\hbar\omega/2k_BT) \approx 2k_BT/\hbar\omega$) limits. Hence from Eq. (74) we see that, effectively, the contribution of the Bogoliubov modes to the MSD behavior in this case is just to modify the mass of the free particle.

In case 2 (coupling to the spin mode), analytical expressions for the Eq. (72) cannot be found. We remind again that we are interested in the transient effects attributed to the bath frequencies right above the band gap, after making the assumption for $\omega = E_{gap} + \epsilon$ that $\omega \approx E_{\mathrm{gap}}$ i.e. $\epsilon \ll E_{\mathrm{gap}}$. In this case the Green function reads as in Eq. (50), while the noise kernel at low temperatures, where $\coth\left(\frac{\hbar\omega}{2k_BT}\right) \to 1$, can be shown to be equal to

$$\begin{aligned}\nu(t) &= \tau_+ (\Lambda - E_{\mathrm{gap}})^{1.5} \\ &\times \left[\frac{2}{3}\cos(E_{\mathrm{gap}} t) F_{1,2}\left(\frac{3}{4}; \frac{1}{2}, \frac{7}{4}; -\frac{1}{4}t^2 (E_{\mathrm{gap}} - \Lambda)^2\right) \right. \\ &+ \frac{2}{5} t (E_{\mathrm{gap}} - \Lambda)\cos(E_{\mathrm{gap}} t) \\ &\left. \times F_{1,2}\left(\frac{5}{4}; \frac{3}{2}, \frac{9}{4}; -\frac{1}{4}t^2 (E_{\mathrm{gap}} - \Lambda)^2\right) \right], \end{aligned} \tag{75}$$

where

$$F_{1,2}(\alpha; \beta, \gamma; z) = \sum_{n=0}^{\infty} \frac{(\alpha)_n}{(\beta)_n (\gamma)_n} \frac{z^n}{n!}. \tag{76}$$

In this case, we were not able to obtain an analytic solution for the MSD. We evaluate it numerically, with the results being valid for finite Ω, as we used the simplified version of the spectral density, Eq. (50). In all calculations we checked that all assumptions made are fulfilled.

In Fig. 3 we show the numerically evaluated MSD as a function of time according to Eq. (72) and different Rabi frequencies and interaction strengths. We remind that initially, $\langle \dot{x}^2(0)\rangle = 0$. In Fig. 3 (a) we show how decreasing Ω both enlarges the duration of

the subdiffusive plateau and reduces the anomalous exponent α. We should note that the results are valid only for finite Ω: since we use the simplifies spectral density, Eq. (50), we are never able to describe the smooth transition to the cubic spectral density, which will show an smooth change to ballistic behavior for the whole range. Then, the effect of reducing Ω is merely to reduce the gap, not to change the form of the spectral density. As a consequence, the plateau is enlarged. In Fig. 3 (b) we show how the MSD varies as a function of the coupling stength of the impurity to the BECs. Here, we observe that increasing the coupling strength results in more subdiffusive motion and an increase in the duration of the subdiffusive plateau. Furthermore, note that, in Fig. 3, time is measured in units of the inverse of $\bar{\Omega} = 1000\pi Hz$ and hence the transient subdiffusive phenomenon appears in time of the order of ms.

In general, from the results presented in Fig. 3, we numerically find three regimes of behavior for the MSD, and in each regime it behaves as $\mathrm{MSD}(t) \propto t^{\alpha}$, where α is different at each regime. The exponent α is known as the anomalous exponent. In regime (i), there is an initial short time behavior where, as expected, the MSD grows more or less ballistically with time. So here, $\alpha \approx 2$; In regime (ii), there is a plateau where $\alpha < 1$. This is a transient subdiffusive behavior; Finally, in regime (iii), which is the long time behavior, the impurity superdiffuses with $\alpha = 2$. We interpret this behavior as follows: the impurity performs free motion initially. Then after interacting with the large frequencies of the bath, the impurity begins to perform a subdiffusive motion since it screens the part of the spectral density that depends on the square root of the bath modes frequencies. At long times, and after undergoing dissipation for some time, the impurity again effectively only interacts with the lower frequencies of the bath which have zero effect on the motion of the impurity and hence the impurity performs a ballistic motion.

Finally, we comment here that the results of the numerical integrations undertaken to obtain the MSD in this section, indeed appear to agree with the analytical calculations we performed in the previous section. This is to be understood in the following sense. The analytical results of the previous section, implied that the coupling of the impurity to the spin mode, results in the impurity interacting with a bath giving rise to a different spectral density, which intuitively one expects to give a different MSD behaviour. This is indeed what we observe in the results presented in Fig. 3.

6 Conclusions

In this work, we studied the diffusive behavior of an impurity immersed in a coherently coupled two-component BEC, that interacts with both of them through contact interactions. We showed how starting from the standard Hamiltonian that would describe such a scenario, one can recast the problem into that of a quantum Brownian particle diffusing in a bath composed of the Bogoliubov modes of the two-component BEC. We discussed the under certain assumptions and conditions required to obtain this description.

We found that the main difference of this scenario compared to that of the impurity being coupled to a single BEC studied in [35], is that for the scenario of the impurity being coupled differently to the two BECs, namely coupled attractively to one of them and repulsively to the other but with the same magnitude, results in the impurity being coupled to the spin mode of the coherently coupled two-component BEC. This implies that its dynamics is determined by a qualitatively different spectral density. In particular this new spectral density is gapped and subohmic close to the gap. We demonstrate numerically, that such a spectral density gives rise to a transient subdiffusive behavior. Furthermore, we show that this transient effect can be controlled by the magnitude of the Rabi frequency, as well as by the strength with which the impurity couples to the two BECs. These can control the time duration for which this subdiffusive behavior appears. A mechanism for inducing a transient controlled subdiffusion in Brownian motion has been also proposed in [82], but with a completely different way for achieving it and most importantly not considering the system from a microscopic perspective. Moreover, we comment that the setup we studied, thanks to the appearance of this gapped subohmic spectral density, could also serve for simulating quantum-optical phenomena, that could be seen for example in photonic crystals, using instead cold atoms, as was proposed also in [83] for the case of optical lattices. In addition, we note that our studies could be extended to the scenario of having two impurities in the coherently coupled two-component BEC, and study as in [37], the effects that the coupling to the spin mode could have on the bath-induced entanglement between the two impurities. Finally, we could also study the effect that this new gapped spectral density could have on the functioning of the impurity as a probe to measure the temperature of the two-component BEC, as in [84]. Last but not least, it should be noted here that, if one considers the scenario of attractive two-body coupling, i.e. $g_{12} < 0$, and includes the Lee-Huang-Yang corrections to the Hamiltonian, one will obtain the scenario of quantum droplets studied theoretically in [85] and recently proven experimentally in [86] . This we expect to lead in different interesting dynamics for the immersed impurity in the two-component coherently coupled BEC.

Acknowledgments

We (M.L. group) acknowledge the Spanish Ministry MINECO (National Plan 15 Grant: FISICATEAMO No. FIS2016-79508-P, FPI), the Ministry of Education of Spain (FPI Grant BES-2015-071803), EU FEDER, European Social Fund, FundaciÃş Cellex, Generalitat de Catalunya (AGAUR Grant No. 2017 SGR 1341 and CERCA/Program), ERC AdG OSYRIS and NOQIA, EU FETPRO QUIC, and the National Science Centre, Poland-Symfonia Grant No. 2016/20/W/ST4/00314. MAGM acknowledges funding from the Spanish Ministry of Education and Vocational Training (MEFP) through the Beatriz Galindo program 2018 (BEAGAL18/00203).

References

[1] P. HÃď nggi and F. Marchesoni. Introduction: 100years of brownian motion. *Chaos: An Interdisciplinary Journal of Nonlinear Science*, 15 (2):026101, 2005. DOI: 10.1063/1.1895505. URL https://doi.org/10.1063/1.1895505.

[2] I. M. Sokolov and J. Klafter. From diffusion to anomalous diffusion: A century after einsteinâĂŹs brownian motion. *Chaos: An Interdisciplinary Journal of Nonlinear Science*, 15(2): 026103, 2005. DOI: 10.1063/1.1860472. URL https://doi.org/10.1063/1.1860472.

[3] H. Scher and E.W. Montroll. Anomalous transit-time dispersion in amorphous solids. *Phys. Rev. B*, 12:2455–2477, Sep 1975. DOI: 10.1103/PhysRevB.12.2455. URL https://link.aps.org/doi/10.1103/PhysRevB.12.2455.

[4] A. Bunde and S. Havlin. *Fractals in science*. Springer-Verlag Berlin Heidelberg, 1994. DOI: 10.1007/978-3-662-11777-4.

[5] M J Saxton. Lateral diffusion in an archipelago. single-particle diffusion. *Biophys J*, 64, 1993. DOI: 10.1016/S0006-3495(93)81548-0. URL https://www.ncbi.nlm.nih.gov/pubmed/8369407.

[6] M. J. Saxton. Single-particle tracking: the distribution of diffusion coefficients. *Biophys J*, 72, 1997. DOI: 10.1016/S0006-3495(97)78820-9. URL https://www.ncbi.nlm.nih.gov/pubmed/9083678.

[7] F. Leyvraz, J. Adler, A. Aharony, A. Bunde, A. Coniglio, D.C. Hong, H.E. Stanley, and D. Stauffer. The random normal superconductor mixture in one dimension. *Journal of Physics A: Mathematical and General*, 19 (17):3683–3692, dec 1986. DOI: 10.1088/0305-4470/19/17/030. URL https://doi.org/10.1088%2F0305-4470%2F19%2F17%2F030.

[8] S. Hottovy, G. Volpe, and J. Wehr. Noise-induced drift in stochastic differential equations with arbitrary friction and diffusion in the smoluchowski-kramers limit. *Journal of Statistical Physics*, 146(4):762–773, Feb 2012. ISSN 1572-9613. DOI: 10.1007/s10955-012-0418-9. URL https://doi.org/10.1007/s10955-012-0418-9.

[9] A.G. Cherstvy and R. Metzler. Population splitting, trapping, and non-ergodicity in heterogeneous diffusion processes. *Phys. Chem. Chem. Phys.*, 15:20220–20235, 2013. DOI: 10.1039/C3CP53056F. URL http://dx.doi.org/10.1039/C3CP53056F.

[10] A.G. Cherstvy, A.V. Chechkin, and R. Metzler. Anomalous diffusion and ergodicity breaking in heterogeneous diffusion processes. *New Journal of Physics*, 15(8): 083039, aug 2013. DOI: 10.1088/1367-2630/15/8/083039. URL https://doi.org/10.1088%2F1367-2630%2F15%2F8%2F083039.

[11] A.G. Cherstvy, A.V. Chechkin, and R. Metzler. Particle invasion, survival, and non-ergodicity in 2d diffusion processes with space-dependent diffusivity. *Soft Matter*, 10:1591–1601, 2014. DOI: 10.1039/C3SM52846D. URL http://dx.doi.org/10.1039/C3SM52846D.

[12] P. Massignan, C. Manzo, J. A. Torreno-Pina, M. F. García-Parajo, M. Lewenstein, and G. J. Lapeyre. Nonergodic subdiffusion from brownian motion in an inhomogeneous medium. *Phys. Rev. Lett.*, 112:150603, Apr 2014. DOI: 10.1103/PhysRevLett.112.150603. URL https://link.aps.org/doi/10.1103/PhysRevLett.112.150603.

[13] Carlo Manzo, Juan A. Torreno-Pina, Pietro Massignan, Gerald J. Lapeyre, Maciej Lewenstein, and Maria F. Garcia Parajo. Weak ergodicity breaking of receptor motion in living cells stemming from random diffusivity. *Phys. Rev. X*, 5:011021, Feb 2015. DOI: 10.1103/PhysRevX.5.011021. URL https://link.aps.org/doi/10.1103/PhysRevX.5.011021.

[14] C. Charalambous, G. Muñoz Gil, A. Celi, M. F. Garcia-Parajo, M. Lewenstein, C. Manzo, and M. A. García-March. Nonergodic subdiffusion from transient interactions with heterogeneous partners. *Phys. Rev. E*, 95: 032403, Mar 2017. DOI: 10.1103/PhysRevE.95.032403. URL https://link.aps.org/doi/10.1103/PhysRevE.95.032403.

[15] B. Min, T. Li, M. Rosenkranz, and W. Bao. Subdiffusive spreading of a bose-einstein condensate in random potentials. *Phys. Rev. A*, 86:053612, Nov 2012. DOI: 10.1103/PhysRevA.86.053612. URL https://link.aps.org/doi/10.1103/PhysRevA.86.053612.

[16] G. Roati, C. DâĂŹErrico, L. Fallani, M. Fattori, C. Fort, M. Zaccanti, G. Modugno, M. Modugno, and M. Inguscio. Anderson localization of a non-interacting boseâĂŞeinstein condensate. *Na-*

ture, 453, 2008. DOI: 10.1038/nature07071. URL https://doi.org/10.1038/nature07071.

[17] F. Jendrzejewski, A. Bernard, K. MÃijller, P. Cheinet, V. Josse, M. Piraud, L. PezzÃľ, L. Sanchez-Palencia, A. Aspect, and P. Bouyer. Three-dimensional localization of ultracold atoms in an optical disordered potential. *Nature Physics*, 8, 2012. DOI: 10.1038/nphys2256. URL https://doi.org/10.1038/nphys2256.

[18] L. Sanchez-Palencia and M. Lewenstein. Disordered quantum gases under control. *Nature Physics*, 6, 2010. DOI: 10.1038/nphys1507. URL https://doi.org/10.1038/nphys1507.

[19] G. Modugno. Anderson localization in bose–einstein condensates. *Reports on Progress in Physics*, 73(10):102401, sep 2010. DOI: 10.1088/0034-4885/73/10/102401. URL https://doi.org/10.1088%2F0034-4885%2F73%2F10%2F102401.

[20] J. Billy, V. Josse, Z. Zuo, A. Bernard, B. Hambrecht, P. Lugan, D. ClÃľment, L. Sanchez-Palencia, P. Bouyer, and A. Aspect. Direct observation of anderson localization of matter waves in a controlled disorder. *Nature*, 453, 2008. DOI: 10.1038/nature07000. URL https://doi.org/10.1038/nature07000.

[21] B. Deissler, M. Zaccanti, G. Roati, C. DâĂŹErrico, M. Fattori, M. Modugno, G. Modugno, and M. Inguscio. Delocalization of a disordered bosonic system by repulsive interactions. *Nature Physics*, 6, 2010. DOI: 10.1038/nphys1635. URL https://doi.org/10.1038/nphys1635.

[22] E. Lucioni, B. Deissler, L. Tanzi, G. Roati, M. Zaccanti, M. Modugno, M. Larcher, F. Dalfovo, M. Inguscio, and G. Modugno. Observation of subdiffusion in a disordered interacting system. *Phys. Rev. Lett.*, 106: 230403, Jun 2011. DOI: 10.1103/PhysRevLett.106.230403. URL https://link.aps.org/doi/10.1103/PhysRevLett.106.230403.

[23] Stefan Donsa, Harald Hofstätter, Othmar Koch, Joachim Burgdörfer, and Iva Březinová. Long-time expansion of a bose-einstein condensate: Observability of anderson localization. *Phys. Rev. A*, 96: 043630, Oct 2017. DOI: 10.1103/PhysRevA.96.043630. URL https://link.aps.org/doi/10.1103/PhysRevA.96.043630.

[24] D. L. Shepelyansky. Delocalization of quantum chaos by weak nonlinearity. *Phys. Rev. Lett.*, 70:1787–1790, Mar 1993. DOI: 10.1103/PhysRevLett.70.1787. URL https://link.aps.org/doi/10.1103/PhysRevLett.70.1787.

[25] G. Kopidakis, S. Komineas, S. Flach, and S. Aubry. Absence of wave packet diffusion in disordered nonlinear systems. *Phys. Rev. Lett.*, 100:084103, Feb 2008. DOI: 10.1103/PhysRevLett.100.084103. URL https://link.aps.org/doi/10.1103/PhysRevLett.100.084103.

[26] A. S. Pikovsky and D. L. Shepelyansky. Destruction of anderson localization by a weak nonlinearity. *Phys. Rev. Lett.*, 100: 094101, Mar 2008. DOI: 10.1103/PhysRevLett.100.094101. URL https://link.aps.org/doi/10.1103/PhysRevLett.100.094101.

[27] S. Flach, D. O. Krimer, and Ch. Skokos. Universal spreading of wave packets in disordered nonlinear systems. *Phys. Rev. Lett.*, 102:024101, Jan 2009. DOI: 10.1103/PhysRevLett.102.024101. URL https://link.aps.org/doi/10.1103/PhysRevLett.102.024101.

[28] Ch. Skokos, D. O. Krimer, S. Komineas, and S. Flach. Delocalization of wave packets in disordered nonlinear chains. *Phys. Rev. E*, 79:056211, May 2009. DOI: 10.1103/PhysRevE.79.056211. URL https://link.aps.org/doi/10.1103/PhysRevE.79.056211.

[29] Hagar Veksler, Yevgeny Krivolapov, and Shmuel Fishman. Spreading for the generalized nonlinear schrödinger equation with disorder. *Phys. Rev. E*, 80:037201, Sep 2009. DOI: 10.1103/PhysRevE.80.037201. URL https://link.aps.org/doi/10.1103/PhysRevE.80.037201.

[30] M. Mulansky and A. Pikovsky. Spreading in disordered lattices with different nonlinearities. *EPL (Europhysics Letters)*, 90 (1):10015, apr 2010. DOI: 10.1209/0295-5075/90/10015. URL https://doi.org/10.1209%2F0295-5075%2F90%2F10015.

[31] T. V. Laptyeva, J. D. Bodyfelt, D. O. Krimer, Ch. Skokos, and S. Flach. The crossover from strong to weak chaos for nonlinear waves in disordered systems. *EPL (Europhysics Letters)*, 91(3):30001, aug 2010. DOI: 10.1209/0295-5075/91/30001. URL https://doi.org/10.1209%2F0295-5075%2F91%2F30001.

[32] A. Iomin. Subdiffusion in the nonlinear schrödinger equation with disorder. *Phys. Rev. E*, 81:017601, Jan 2010. DOI: 10.1103/PhysRevE.81.017601. URL https://link.aps.org/doi/10.1103/PhysRevE.81.017601.

[33] M. Larcher, F. Dalfovo, and M. Modugno. Effects of interaction on the diffusion of atomic matter waves in one-dimensional quasiperiodic potentials. *Phys. Rev. A*, 80: 053606, Nov 2009. DOI: 10.1103/PhysRevA.80.053606. URL https://link.aps.org/doi/10.1103/PhysRevA.80.053606.

[34] L.M. Aycock, H.M. Hurst, D.K. Efimkin, D. Genkina, H.-I. Lu, V.M. Galitski, and I. B. Spielman. Brownian motion of solitons in a bose–einstein condensate. *Proceedings of the National Academy of Sciences*, 114 (10):2503–2508, 2017. ISSN 0027-8424. DOI:

10.1073/pnas.1615004114. URL https://www.pnas.org/content/114/10/2503.

[35] A. Lampo, S.H. Lim, M.A. García-March, and M. Lewenstein. Bose polaron as an instance of quantum Brownian motion. *Quantum*, 1: 30, September 2017. ISSN 2521-327X. DOI: 10.22331/q-2017-09-27-30. URL https://doi.org/10.22331/q-2017-09-27-30.

[36] A. Lampo, C. Charalambous, M.A. García-March, and M. Lewenstein. Non-markovian polaron dynamics in a trapped bose-einstein condensate. *Phys. Rev. A*, 98:063630, Dec 2018. DOI: 10.1103/PhysRevA.98.063630. URL https://link.aps.org/doi/10.1103/PhysRevA.98.063630.

[37] C. Charalambous, M.A. Garcia-March, A. Lampo, M. Mehboudi, and M. Lewenstein. Two distinguishable impurities in BEC: squeezing and entanglement of two Bose polarons. *SciPost Phys.*, 6:10, 2019. DOI: 10.21468/SciPostPhys.6.1.010. URL https://scipost.org/10.21468/SciPostPhys.6.1.010.

[38] D.K. Efimkin, J. Hofmann, and V. Galitski. Non-markovian quantum friction of bright solitons in superfluids. *Phys. Rev. Lett.*, 116:225301, May 2016. DOI: 10.1103/PhysRevLett.116.225301. URL https://link.aps.org/doi/10.1103/PhysRevLett.116.225301.

[39] H.M. Hurst, D.K. Efimkin, I. B. Spielman, and V. Galitski. Kinetic theory of dark solitons with tunable friction. *Phys. Rev. A*, 95:053604, May 2017. DOI: 10.1103/PhysRevA.95.053604. URL https://link.aps.org/doi/10.1103/PhysRevA.95.053604.

[40] A. Cem Keser and V. Galitski. Analogue stochastic gravity in strongly-interacting boseâĂŞeinstein condensates. *Annals of Physics*, 395: 84 – 111, 2018. ISSN 0003-4916. DOI: https://doi.org/10.1016/j.aop.2018.05.009. URL http://www.sciencedirect.com/science/article/pii/S0003491618301453.

[41] Julius Bonart and Leticia F. Cugliandolo. From nonequilibrium quantum brownian motion to impurity dynamics in one-dimensional quantum liquids. *Phys. Rev. A*, 86:023636, Aug 2012. DOI: 10.1103/PhysRevA.86.023636. URL https://link.aps.org/doi/10.1103/PhysRevA.86.023636.

[42] X.-D. Bai and J.-K. Xue. Subdiffusion of dipolar gas in one-dimensional quasiperiodic potentials. *Chinese Physics Letters*, 32 (1):010302, jan 2015. DOI: 10.1088/0256-307x/32/1/010302. URL https://doi.org/10.1088%2F0256-307x%2F32%2F1%2F010302.

[43] K.-T. Xi, J. Li, and D.-N. Shi. Localization of a two-component boseâĂŞeinstein condensate in a two-dimensional bichromatic optical lattice. *Physica B: Condensed Matter*, 436: 149 – 156, 2014. ISSN 0921-4526. DOI: https://doi.org/10.1016/j.physb.2013.12.010. URL http://www.sciencedirect.com/science/article/pii/S0921452613007837.

[44] Y. Ashida, R. Schmidt, L. Tarruell, and E. Demler. Many-body interferometry of magnetic polaron dynamics. *Phys. Rev. B*, 97:060302, Feb 2018. DOI: 10.1103/PhysRevB.97.060302. URL https://link.aps.org/doi/10.1103/PhysRevB.97.060302.

[45] A.J. Leggett. Bose-einstein condensation in the alkali gases: Some fundamental concepts. *Rev. Mod. Phys.*, 73:307–356, Apr 2001. DOI: 10.1103/RevModPhys.73.307. URL https://link.aps.org/doi/10.1103/RevModPhys.73.307.

[46] K. B. Davis, M. O. Mewes, M. R. Andrews, N. J. van Druten, D. S. Durfee, D. M. Kurn, and W. Ketterle. Bose-einstein condensation in a gas of sodium atoms. *Phys. Rev. Lett.*, 75:3969–3973, Nov 1995. DOI: 10.1103/PhysRevLett.75.3969. URL https://link.aps.org/doi/10.1103/PhysRevLett.75.3969.

[47] C. J. Myatt, E. A. Burt, R. W. Ghrist, E. A. Cornell, and C. E. Wieman. Production of two overlapping bose-einstein condensates by sympathetic cooling. *Phys. Rev. Lett.*, 78:586–589, Jan 1997. DOI: 10.1103/PhysRevLett.78.586. URL https://link.aps.org/doi/10.1103/PhysRevLett.78.586.

[48] D. M. Stamper-Kurn, M. R. Andrews, A. P. Chikkatur, S. Inouye, H.-J. Miesner, J. Stenger, and W. Ketterle. Optical confinement of a bose-einstein condensate. *Phys. Rev. Lett.*, 80: 2027–2030, Mar 1998. DOI: 10.1103/PhysRevLett.80.2027. URL https://link.aps.org/doi/10.1103/PhysRevLett.80.2027.

[49] H.-J. Miesner, D. M. Stamper-Kurn, J. Stenger, S. Inouye, A. P. Chikkatur, and W. Ketterle. Observation of metastable states in spinor bose-einstein condensates. *Phys. Rev. Lett.*, 82: 2228–2231, Mar 1999. DOI: 10.1103/PhysRevLett.82.2228. URL https://link.aps.org/doi/10.1103/PhysRevLett.82.2228.

[50] J. Stenger, S. Inouye, D. M. Stamper-Kurn, H.-J. Miesner, A. P. Chikkatur, and W. Ketterle. Spin domains in ground-state boseâĂŞeinstein condensates. *Nature*, 396:345–348, 1998. DOI: 10.1038/24567. URL https://doi.org/10.1038/24567.

[51] M. R. Matthews, D. S. Hall, D. S. Jin, J. R. Ensher, C. E. Wieman, E. A. Cornell, F. Dalfovo, C. Minniti, and S. Stringari. Dynamical response of a bose-einstein condensate to a discontinuous change in internal state. *Phys. Rev. Lett.*, 81:243–247, Jul 1998. DOI: 10.1103/PhysRevLett.81.243. URL https://link.aps.org/doi/10.1103/PhysRevLett.81.243.

[52] D. S. Petrov, G. V. Shlyapnikov, and J. T. M. Walraven. Regimes of quantum degeneracy in trapped 1d gases. *Phys. Rev. Lett.*, 85: 3745–3749, Oct 2000. DOI: 10.1103/PhysRevLett.85.3745. URL https://link.aps.org/doi/10.1103/PhysRevLett.85.3745.

[53] P. Tommasini, E. J. V. de Passos, A. F. R. de Toledo Piza, M. S. Hussein, and E. Timmermans. Bogoliubov theory for mutually coherent condensates. *Phys. Rev. A*, 67:023606, Feb 2003. DOI: 10.1103/PhysRevA.67.023606. URL https://link.aps.org/doi/10.1103/PhysRevA.67.023606.

[54] S. Lellouch, T.-L. Dao, T. Koffel, and L. Sanchez-Palencia. Two-component bose gases with one-body and two-body couplings. *Phys. Rev. A*, 88:063646, Dec 2013. DOI: 10.1103/PhysRevA.88.063646. URL https://link.aps.org/doi/10.1103/PhysRevA.88.063646.

[55] M. Abad and A. Recati. A study of coherently coupled two-component bose-einstein condensates. *The European Physical Journal D*, 67(7):148, Jul 2013. ISSN 1434-6079. DOI: 10.1140/epjd/e2013-40053-2. URL https://doi.org/10.1140/epjd/e2013-40053-2.

[56] G.-S. Paraoanu, S. Kohler, F. Sols, and A.J. Leggett. The josephson plasmon as a bogoliubov quasiparticle. *Journal of Physics B: Atomic, Molecular and Optical Physics*, 34(23): 4689–4696, nov 2001. DOI: 10.1088/0953-4075/34/23/313. URL https://doi.org/10.1088%2F0953-4075%2F34%2F23%2F313.

[57] A. Recati and F. Piazza. Breaking of goldstone modes in a two-component bose-einstein condensate. *Phys. Rev. B*, 99: 064505, Feb 2019. DOI: 10.1103/PhysRevB.99.064505. URL https://link.aps.org/doi/10.1103/PhysRevB.99.064505.

[58] E. Nicklas. A new tool for miscibility control: Linear coupling. 01 2013.

[59] S. John and T. Quang. Spontaneous emission near the edge of a photonic band gap. *Phys. Rev. A*, 50:1764–1769, Aug 1994. DOI: 10.1103/PhysRevA.50.1764. URL https://link.aps.org/doi/10.1103/PhysRevA.50.1764.

[60] H.-T. Tan, W.-M. Zhang, and G.-x. Li. Entangling two distant nanocavities via a waveguide. *Phys. Rev. A*, 83:062310, Jun 2011. DOI: 10.1103/PhysRevA.83.062310. URL https://link.aps.org/doi/10.1103/PhysRevA.83.062310.

[61] J. Prior, I. de Vega, A.W. Chin, S.F. Huelga, and M.B. Plenio. Quantum dynamics in photonic crystals. *Phys. Rev. A*, 87:013428, Jan 2013. DOI: 10.1103/PhysRevA.87.013428. URL https://link.aps.org/doi/10.1103/PhysRevA.87.013428.

[62] A.G. Kofman, G. Kurizki, and B. Sherman. Spontaneous and induced atomic decay in photonic band structures. *Journal of Modern Optics*, 41(2):353–384, 1994. DOI: 10.1080/09500349414550381. URL https://doi.org/10.1080/09500349414550381.

[63] V. P Bykov. Spontaneous emission in a periodic structure. *Journal of Experimental and Theoretical Physics*, 35:269, 01 1972.

[64] E. Yablonovitch. Inhibited spontaneous emission in solid-state physics and electronics. *Phys. Rev. Lett.*, 58:2059–2062, May 1987. DOI: 10.1103/PhysRevLett.58.2059. URL https://link.aps.org/doi/10.1103/PhysRevLett.58.2059.

[65] P. Lambropoulos, G.M. Nikolopoulos, T.R. Nielsen, and S. Bay. Fundamental quantum optics in structured reservoirs. *Reports on Progress in Physics*, 63(4):455–503, mar 2000. DOI: 10.1088/0034-4885/63/4/201. URL https://doi.org/10.1088%2F0034-4885%2F63%2F4%2F201.

[66] M. Woldeyohannes and S. John. Coherent control of spontaneous emission near a photonic band edge. *Journal of Optics B: Quantum and Semiclassical Optics*, 5(2): R43–R82, feb 2003. DOI: 10.1088/1464-4266/5/2/201. URL https://doi.org/10.1088%2F1464-4266%2F5%2F2%2F201.

[67] T. Quang, M. Woldeyohannes, S. John, and G.S. Agarwal. Coherent control of spontaneous emission near a photonic band edge: A single-atom optical memory device. *Phys. Rev. Lett.*, 79:5238–5241, Dec 1997. DOI: 10.1103/PhysRevLett.79.5238. URL https://link.aps.org/doi/10.1103/PhysRevLett.79.5238.

[68] A. G. Kofman and G. Kurizki. Unified theory of dynamically suppressed qubit decoherence in thermal baths. *Phys. Rev. Lett.*, 93:130406, Sep 2004. DOI: 10.1103/PhysRevLett.93.130406. URL https://link.aps.org/doi/10.1103/PhysRevLett.93.130406.

[69] H.P. Breuer and F. Petruccione. *The Theory of Open Quantum Systems*. OUP Oxford, 2007. ISBN 9780199213900. URL https://books.google.es/books?id=DkcJPwAACAAJ.

[70] A. Rivas, A. Douglas K. Plato, S.F. Huelga, and M.B. Plenio. Markovian master equations: a critical study. *New Journal of Physics*, 12 (11):113032, nov 2010. DOI: 10.1088/1367-2630/12/11/113032. URL https://doi.org/10.1088%2F1367-2630%2F12%2F11%2F113032.

[71] I. de Vega, D. Alonso, and P. Gaspard. Two-level system immersed in a photonic band-gap material: A non-markovian stochastic schrödinger-equation approach. *Phys. Rev. A*, 71:023812, Feb 2005. DOI: 10.1103/PhysRevA.71.023812. URL https://link.aps.org/doi/10.1103/PhysRevA.71.023812.

[72] I. de Vega, D. Porras, and I.J. Cirac. Matter-wave emission in optical lattices: Single particle and collective effects. *Phys. Rev. Lett.*, 101:260404, Dec 2008. DOI: 10.1103/PhysRevLett.101.260404. URL https://link.aps.org/doi/10.1103/PhysRevLett.101.260404.

[73] R. Vasile, F. Galve, and R. Zambrini. Spectral origin of non-markovian open-system dynamics: A finite harmonic model without approximations. *Phys. Rev. A*, 89: 022109, Feb 2014. DOI: 10.1103/PhysRevA.89.022109. URL https://link.aps.org/doi/10.1103/PhysRevA.89.022109.

[74] W.-M. Zhang, P.-Y. Lo, H.-N. Xiong, M. W.-Y. Tu, and F. Nori. General non-markovian dynamics of open quantum systems. *Phys. Rev. Lett.*, 109:170402, Oct 2012. DOI: 10.1103/PhysRevLett.109.170402. URL https://link.aps.org/doi/10.1103/PhysRevLett.109.170402.

[75] F. Giraldi and F. Petruccione. Fractional relaxations in photonic crystals. *Journal of Physics A: Mathematical and Theoretical*, 47 (39):395304, sep 2014. DOI: 10.1088/1751-8113/47/39/395304. URL https://doi.org/10.1088%2F1751-8113%2F47%2F39%2F395304.

[76] M. Bruderer, A. Klein, S.R. Clark, and D. Jaksch. Polaron physics in optical lattices. *Phys. Rev. A*, 76:011605, Jul 2007. DOI: 10.1103/PhysRevA.76.011605. URL https://link.aps.org/doi/10.1103/PhysRevA.76.011605.

[77] S. Patrick Rath and R. Schmidt. Field-theoretical study of the bose polaron. *Phys. Rev. A*, 88:053632, Nov 2013. DOI: 10.1103/PhysRevA.88.053632. URL https://link.aps.org/doi/10.1103/PhysRevA.88.053632.

[78] R.S. Christensen, J. Levinsen, and G.M. Bruun. Quasiparticle properties of a mobile impurity in a bose-einstein condensate. *Phys. Rev. Lett.*, 115:160401, Oct 2015. DOI: 10.1103/PhysRevLett.115.160401. URL https://link.aps.org/doi/10.1103/PhysRevLett.115.160401.

[79] Y.E. Shchadilova, R. Schmidt, F. Grusdt, and E. Demler. Quantum dynamics of ultracold bose polarons. *Phys. Rev. Lett.*, 117:113002, Sep 2016. DOI: 10.1103/PhysRevLett.117.113002. URL https://link.aps.org/doi/10.1103/PhysRevLett.117.113002.

[80] Q. Wang and H. Zhan. On different numerical inverse laplace methods for solute transport problems. *Advances in Water Resources*, 75:80 – 92, 2015. ISSN 0309-1708. DOI: https://doi.org/10.1016/j.advwatres.2014.11.001. URL http://www.sciencedirect.com/science/article/pii/S0309170814002152.

[81] P.-Y. Lo, H.-N. Xiong, and W.-M. Zhang. Breakdown of bose-einstein distribution in photonic crystals. *Scientific Reports*, 5, 2015. DOI: 10.1038/srep09423. URL https://doi.org/10.1038/srep09423.

[82] J. Spiechowicz, J. ÅĄuczka, and P. HÃďnggi. Transient anomalous diffusion in periodic systems: ergodicity, symmetry breaking and velocity relaxation. *Scientific Reports*, 6, 2016. DOI: 10.1038/srep30948. URL https://doi.org/10.1038/srep30948.

[83] C. Navarrete-Benlloch, I. de Vega, D. Porras, and J.I. Cirac. Simulating quantum-optical phenomena with cold atoms in optical lattices. *New Journal of Physics*, 13 (2):023024, feb 2011. DOI: 10.1088/1367-2630/13/2/023024. URL https://doi.org/10.1088%2F1367-2630%2F13%2F2%2F023024.

[84] M. Mehboudi, A. Lampo, C. Charalambous, L.A. Correa, M.Á. García-March, and M. Lewenstein. Using polarons for sub-nk quantum nondemolition thermometry in a bose-einstein condensate. *Phys. Rev. Lett.*, 122:030403, Jan 2019. DOI: 10.1103/PhysRevLett.122.030403. URL https://link.aps.org/doi/10.1103/PhysRevLett.122.030403.

[85] D. S. Petrov. Quantum mechanical stabilization of a collapsing bose-bose mixture. *Phys. Rev. Lett.*, 115:155302, Oct 2015. DOI: 10.1103/PhysRevLett.115.155302. URL https://link.aps.org/doi/10.1103/PhysRevLett.115.155302.

[86] C. R. Cabrera, L. Tanzi, J. Sanz, B. Naylor, P. Thomas, P. Cheiney, and L. Tarruell. Quantum liquid droplets in a mixture of bose-einstein condensates. *Science*, 359(6373):301–304, 2018. ISSN 0036-8075. DOI: 10.1126/science.aao5686. URL https://science.sciencemag.org/content/359/6373/301.